

# Calibrate and Debias Layer-wise Sampling for Graph Convolutional Networks

Yifan Chen\*   Tianning Xu\*  
*University of Illinois Urbana-Champaign*

Dilek Hakkani-Tur   Di Jin  
*Amazon Alexa AI*

Yun Yang   Ruoqing Zhu  
*University of Illinois Urbana-Champaign*

## Abstract

To accelerate the training of graph convolutional networks (GCNs), many sampling-based methods have been developed for approximating the embedding aggregation. Among them, a layer-wise approach recursively performs importance sampling to select neighbors jointly for existing nodes in each layer. This paper revisits the approach from a matrix approximation perspective. We identify two issues in the existing layer-wise sampling methods: sub-optimal sampling probabilities and the approximation bias induced by sampling without replacement. We propose two remedies: new sampling probabilities and a debiasing algorithm, to address these issues, and provide the statistical analysis of the estimation variance. The improvements are demonstrated by extensive analyses and experiments on common benchmarks.

## 1 Introduction

Graph Convolutional Networks (Kipf & Welling, 2017) are popular methods for learning the representation of nodes. However, it is computationally challenging to train a GCN over large-scale graphs due to the inter-dependence of nodes in a graph. In the mini-batch training for an  $L$ -layer GCN, the computation of embeddings involves not only the batch nodes but also the batch nodes’  $L$ -hop neighbors, which is known as the phenomenon of “neighbor explosion” (Zeng et al., 2019) or “neighbor expansion” (Chen et al., 2018a; Huang et al., 2018). To alleviate such a computation issue for large graphs, sampling-based methods are proposed to accelerate the training and reduce the memory cost. These approaches can be categorized as node-wise sampling approaches (Hamilton et al., 2017; Chen et al., 2018a), subgraph sampling approaches (Zeng et al., 2019; Chiang et al., 2019; Cong et al., 2020), and layer-wise sampling approaches (Chen et al., 2018b; Huang et al., 2018; Zou et al., 2019). We focus on layer-wise sampling in this work, which enjoys the efficiency and variance reduction by sampling columns of renormalized Laplacian matrix in each layer.

This paper is a revisit of the existing sampling schemes in layer-wise sampling methods. We identify two potential drawbacks in the common practice for layer-wise sampling (Chen et al., 2018b; Zou et al., 2019). First, the sampling probabilities are sub-optimal since a core assumption in FastGCN and LADIES does not hold in many common graph benchmarks, such as Reddit (Hamilton et al., 2017) and OGB (Hu et al., 2020). Secondly, the previous implementations of the layer-wise sampling methods perform sampling without replacement, which deviates from their theoretical results, and introduce biases in the estimation. Realizing the two issues, we accordingly propose the remedies with new sampling probabilities and a debiasing algorithm, and the variance analyses for the two propositions are provided as well. The empirical improvements of the proposed methods are demonstrated by extensive experiments with evaluating the matrix approximation error and prediction accuracy on large-scale benchmarks.

\* Equal contribution. The majority of this work was done prior to the first author’s internship at Amazon Alexa AI.

To the best of our knowledge, our result is the first to recognize and resolve the issues with the default assumption and the practical implementation of layer-wise sampling methods for GCN. Once these sub-optimal practices are addressed, we observe that the GCN models consistently converge faster in training and tend to enjoy a higher prediction accuracy. We believe the proposed methods can more generally improve the training for GCN as well, e.g., the same strategy can allow node-wise sampling methods to adopt importance sampling without replacement and further improve the approximation accuracy. Moreover, our discussion on the bias induced by sampling without replacement is not limited to GCN, and the debiasing algorithm we develop can contribute to other sampling-based machine learning models beyond layer-wise sampling.

## 1.1 Background and Related Work

**GCN.** Graph Convolutional Networks (GCNs, Kipf & Welling (2017)) effectively incorporate the technique of convolution filter into the graph domain (Wu et al., 2020; Bronstein et al., 2017). Viewed as an approximation for the spectral graph convolutions (Bruna et al., 2014; Defferrard et al., 2016), GCN has achieved great success in learning tasks such as node classification and link prediction, with applications ranging from recommender systems (Ying et al., 2018), traffic prediction (Cui et al., 2019; Rahimi et al., 2018), and knowledge graphs (Schlichtkrull et al., 2018).

**Sampling-based GCN Training.** To name a few of sampling schemes, GraphSAGE (Hamilton et al., 2017) first introduces the “node-wise” neighbor sampling scheme, where a fixed number of neighbors are uniformly and independently sampled for each node in every layer. To reduce variance in node-wise sampling training, VR-GCN (Chen et al., 2018a) applies a control variate based algorithm using historical activation. Instead of sampling for each node separately, “layer-wise” sampling is a more efficient approach: joint sampling scheme for all the existing nodes in each layer so that these nodes can share the sampled neighboring node. FastGCN (Chen et al., 2018b) first introduces this scheme with importance sampling. AS-GCN (Huang et al., 2018) proposes an alternative sampling probability for layer-wise sampling by approximating the hidden layer in the sampling procedure. Then Zou et al. (2019) propose a layer-dependent importance sampling scheme (LADIES) to further reduce the variance in training. This alleviates the issue of empty rows in the sampled adjacency matrix of FastGCN. Besides, as the “subgraph” approaches, ClusterGCN (Chiang et al., 2019) samples a dense subgraph associated with the batch nodes by graph clustering algorithm; GraphSAINT (Zeng et al., 2019) introduces normalization and variance reduction in subgraph sampling.

## 2 Notations and Preliminaries

### 2.1 Graph Convolutional Networks

The GCN architecture for semi-supervised node classification is introduced by Kipf & Welling (2017). Suppose we have an undirected graph  $\mathcal{G} = (\mathcal{V}, \mathcal{E})$ , where  $\mathcal{V}$  is the set of  $n$  nodes and  $\mathcal{E}$  is the set of  $E$  edges. Denote node  $i$  in  $\mathcal{V}$  as  $v_i$ , where  $i \in [n]$  is the index of nodes in the graph and  $[n]$  denotes the set  $\{1, 2, \dots, n\}$ . Each node  $v_i \in \mathcal{V}$  is associated with a feature vector  $x_i \in \mathbb{R}^p$  and a label vector  $y_i \in \mathbb{R}^q$ . Though we can observe the feature of every node in  $\mathcal{V}$  and every edge in  $\mathcal{E}$ , i.e. the  $n \times n$  adjacency matrix  $A$ , we are only able to observe the label of partial nodes  $\mathcal{V}_{train}$ , satisfying  $\mathcal{V}_{train} \subset \mathcal{V}$ . Thus, we need to predict the labels for the rest nodes in  $\mathcal{V} \setminus \mathcal{V}_{train}$  and it becomes a semi-supervised learning task. A graph convolution layer is defined as:

$$\mathbf{Z}^{(l+1)} = \mathbf{P}\mathbf{H}^{(l)}\mathbf{W}^{(l)}, \quad \mathbf{H}^{(l)} = \sigma(\mathbf{Z}^{(l)}), \quad (1)$$

where  $\sigma$  is an activation function and  $\mathbf{P}$  is obtained from applying normalization to the graph adjacency matrix  $\mathbf{A}$ ;  $\mathbf{H}^{(l)}$  is the embedding matrix of the graph nodes in the  $l$ -th layer, and  $\mathbf{W}^{(l)}$  is the parameter matrix of the same layer. In particular,  $\mathbf{H}^{(0)}$  is the  $n \times p$  feature matrix. For mini-batch training, the training loss for an  $L$ -layer GCN is defined as  $\frac{1}{|\mathcal{V}_{batch}|} \sum_{v_i \in \mathcal{V}_{batch}} \ell(y_i, z_i^{(L)})$ , where  $\ell$  is the loss function, batch nodes  $\mathcal{V}_{batch}$  is a subset of  $\mathcal{V}_{train}$  at each iteration.  $z_i^{(L)}$  is the  $i$ -th row in  $\mathbf{Z}^{(L)}$ ,  $|\cdot|$  denotes the cardinality of a set.

In this paper, we set  $\mathbf{P} = \tilde{\mathbf{D}}^{-1/2}(\mathbf{A} + \mathbf{I})\tilde{\mathbf{D}}^{-1/2}$ , where  $\tilde{\mathbf{D}}$  is a diagonal matrix with  $D_{ii} = 1 + \sum_j A_{ij}$ . The matrix  $\mathbf{P}$  is constructed as a *renormalized Laplacian matrix* to help alleviate overfitting and explod-

ing/vanishing gradients issues (Kipf & Welling, 2017), which is used by Kipf & Welling (2017); Chen et al. (2018a); Cong et al. (2020).

## 2.2 Layer-wise Sampling

To address the “neighbor explosion” issue for graph neural networks, sampling methods are integrated into the stochastic training. Motivated by the idea to approximate the matrix  $\mathbf{P}\mathbf{H}^{(l)}$  in (1), FastGCN (Chen et al., 2018b) applies an importance-sampling-based strategy. Instead of individually sampling neighbors for each node in the  $l$ -th layer, they sample a set of  $s$  neighbors  $\mathcal{S}^{(l)}$  from  $\mathcal{V}$  with importance sampling probability  $p_i$ , where  $p_i \propto \sum_{j=1}^n \mathbf{P}_{ji}^2$  and  $\sum_i p_i = 1$ . For the  $(l-1)$ -th layer, they naturally set  $\mathcal{V}^{(l-1)} = \mathcal{S}^{(l)}$ . LADIES (Zou et al., 2019) improves the importance sampling probability  $p_i$  as

$$p_i^{(l)} \propto \sum_{v_j \in \mathcal{N}^{(l)}} \mathbf{P}_{ji}^2, \forall i \in [n] \quad (2)$$

where  $\mathcal{N}^{(l)} = \cup_{v_i \in \mathcal{V}^{(l)}} \mathcal{N}(v_i)$  and  $\sum_j p_j^{(l)} = 1$ . In this case,  $\mathcal{S}^{(l)}$  the nodes sampled for the  $l$ -th layer are guaranteed to be within the neighborhood of  $\mathcal{V}^{(l)}$ . The whole procedure can be concluded by a diagonal matrix  $\mathbf{S}^{(l)} \in \mathbb{R}^{n \times n}$  and a row selection matrix  $\mathbf{Q}^{(l)} \in \mathbb{R}^{s_l \times n}$ , which are defined as

$$\mathbf{Q}_{k,j}^{(l)} = \begin{cases} 1, & j = i_k^{(l)} \\ 0, & \text{else} \end{cases}, \quad \mathbf{S}_{j,j}^{(l)} = \begin{cases} (s_l p_{i_k^{(l)}}^{(l)})^{-1}, & j = i_k^{(l)} \\ 0, & \text{else,} \end{cases} \quad (3)$$

where  $\{i_k^{(l)}\}_{k=1}^{s_l}$  are the indices of rows selected in the  $l$ -th layer. The forward propagation with layer-wise sampling can thus be equivalently represented as  $\tilde{\mathbf{Z}}^{(l+1)} = \mathbf{Q}^{(l+1)} \mathbf{P} \mathbf{S}^{(l)} \mathbf{H}^{(l)} \mathbf{W}^{(l)}$ ,  $\mathbf{H}^{(l)} = (\mathbf{Q}^{(l)})^T \sigma(\tilde{\mathbf{Z}}^{(l)})$ , where  $\tilde{\mathbf{Z}}^{(l+1)}$  is the approximation of the embedding matrix for layer  $l$ .

## 3 Experimental Setup

In advance of further discussions of existing issues and corresponding remedies in Section 4 and Section 5, we state the basic setups of main experiments and datasets as they appear multiple times across the paper. Details about GCN model training are deferred to the related sections.

**Main experiments.** To study the influence of the aforementioned issues we evaluate the matrix approximation error (c.f. Figure 1) of different methods in one-step propagation. This is an important metric to reflect the performance of the sampling strategy on approximating the original mini-batch training. Since the updates of parameters in the training are not involved in the simple metric above, in Section 6 we further evaluate the prediction accuracy on testing sets of both intermediate models during training and final outputs, using the metrics in Table 1.

Table 1: Summary of datasets. Each undirected edge is counted once. Each node in ogbn-protein has 112 binary labels. “D.” refers to the average degree of the graph. “Feat” refers to the number of features. “Split Ratio” refers to the ratio of training/validation/test data.

Dataset	Nodes	Edges	D.	Feat.	Classes	Tasks	Split Ratio	Metric
Reddit	232,965	11,606,919	50	602	41	1	66/10/24	F1-score
ogbn-arxiv	160,343	1,166,243	13.7	128	40	1	54/18/28	Accuracy
ogbn-proteins	132,534	39,561,252	597.0	8	binary	112	65/16/19	ROC-AUC
ogbn-mag	736,389	5,396,336	7.3	128	349	1	85/9/6	Accuracy
ogbn-products	2,449,029	61,859,140	50.5	100	47	1	8/2/90	Accuracy

**Benchmarks.** Empirical experiments are conducted on 5 datasets (see details in Table 1): Reddit (Hamilton et al., 2017), ogbn-arxiv, ogbn-proteins, ogbn-mag and ogbn-products (Hu et al., 2020). Reddit is a traditional large graph dataset used by Chen et al. (2018b); Zou et al. (2019); Chen et al. (2018a); Cong et al. (2020); Zeng et al. (2019). Ognb-arxiv, ogbn-proteins and ogbn-products are Open Graph Benchmarks (OGB) proposed by Hu et al. (2020). Compared to traditional datasets, our selected OGB data have a larger

volume (up to the million-node scale) with a more challenging data split. The metrics in Table 1 follow the choices of recent works and the recommendation by Hu et al. (2020).

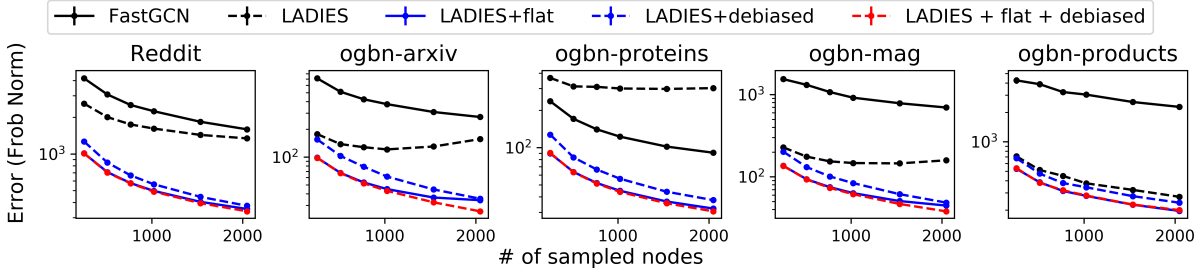


Figure 1: Matrix approximation errors of layer-wise sampling methods. The error curves of LADIES show an abnormal U-shape on ogbn-arxiv and ogbn-mag datasets. “flat” and “debiased” denote our methods in Sections 4 and 5 respectively.

## 4 Reconsider Importance Sampling Probabilities

The efficiency of layer-wise sampling relies on its importance sampling procedure, where the choice of sampling probabilities significantly impacts the prediction accuracy of GCNs. To minimize the following variance (for the sake of notational brevity, from now on we omit the superscript  $(l)$  when the objects are from the same layer)

$$\mathbb{E} \|QPSHW - QPHW\|_F^2, \quad (4)$$

Zou et al. (2019) show that the optimal sampling probability  $p_i$  for node  $i$  satisfies (also see Appendix C.1 for a derivation from a perspective of approximate matrix multiplication)

$$p_i \propto \|(\mathbf{HW})_{[i]}\| \cdot \|\mathbf{QP}^{[i]}\|,$$

where for a matrix  $\mathbf{A}$ ,  $\mathbf{A}_{[i]}$  and  $\mathbf{A}^{[i]}$  respectively represent the  $i$ -th row / column of matrix  $\mathbf{A}$ .

### 4.1 Current Strategies and Their Limitations

The optimal sampling probabilities discussed above are usually unavailable during the mini-batch training. Because  $\mathbf{W}$  and  $\mathbf{H}$  keep changing in the training and even worse we only have access to part of the matrix  $\mathbf{HW}$  in each batch. To approximate the optimal sampling probability, previous works develop two different strategies, 1) approximating the hidden activation  $\mathbf{HW}$ , or 2) sampling without the information from  $\mathbf{HW}$ .

A representative of the former strategy is AS-GCN (Huang et al., 2018), which linearly approximate  $\mathbf{HW}$  by node features. This strategy improves the accuracy of efficient GCN, while the estimation of hidden activation causes considerable overall training time, which in practice can be “even longer than vanilla GCN” (Zeng et al., 2019). Another issue with this strategy is that the approximation must be updated during the training procedure. This dependence between sampling and training, makes it impossible to save training time by preparing sampling results in advance of the training. Hence, this method is not a focus of this paper.

Instead, the second strategy, the theme of our paper, allows the decoupling of sampling and training and has been adopted by FastGCN (Chen et al., 2018b) and LADIES (Zou et al., 2019). To proceed without the information from  $\mathbf{HW}$ , FastGCN (resp. LADIES) assumes  $\|(\mathbf{HW})_{[i]}\| \propto \|\mathbf{P}^{[i]}\|$  (resp.  $\|\mathbf{QP}^{[i]}\|$ ), and sets their sampling probabilities as  $p_i \propto \|\mathbf{P}^{[i]}\|^2$  (resp.  $\|\mathbf{QP}^{[i]}\|^2$ ),  $\forall i \in [n]$ . However, we find this assumption is too strong. To test it, we conduct a linear regression

$$\|(\mathbf{HW})_{[i]}\| \sim \beta_0 + \beta_1 \|\mathbf{P}^{[i]}\|$$



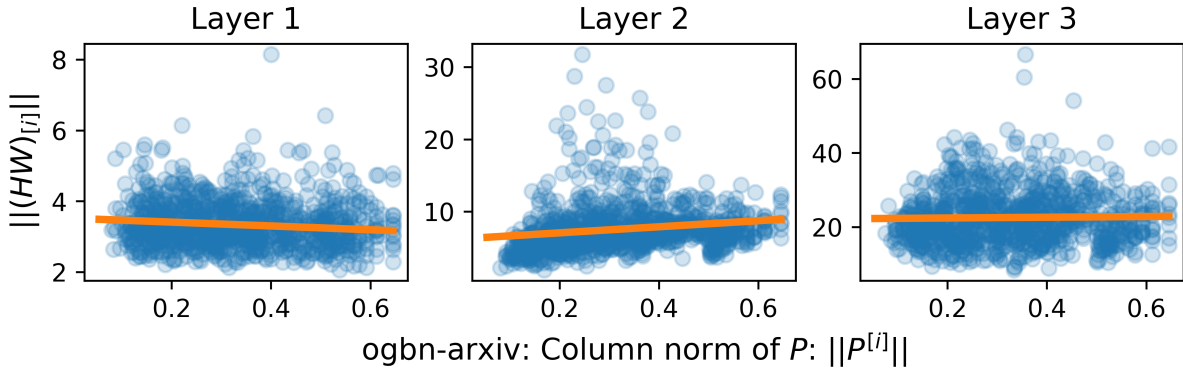


Figure 2: A scatter plot shows the joint distribution of  $\|(HW)_{[i]}\|$  and  $\|P^{[i]}\|$  on ogbn-arxiv dataset. The orange solid lines are the fitted regression line, and the data points are collected from converged 3-layer GCN models in 5 repeated experiments.

Table 2: Regression coefficients on ogbn-arxiv

	Layer 1	Layer 2	Layer 3
$\beta_0$	$3.517(\pm 0.002)$	$6.21(\pm 0.01)$	$22.21(\pm 0.02)$
$\beta_1$	$-0.54(\pm 0.005)$	$4.20(\pm 0.03)$	$1.00(\pm 0.06)$

for each layers separately, where  $\|(HW)_{[i]}\|$  is the  $\ell_2$  norm of a row in  $\mathbf{HW}$  and  $\|P^{[i]}\|$  is the norm of corresponding column in  $\mathbf{P}$ .

We represent the regression results with LADIES on ogbn-arxiv dataset in Table 2 Figure 2. The fitted intercept  $\beta_0$  of the regression lines are much larger than the slope  $\beta_1$  in layer 1 and 3. Moreover, the slope  $\beta_1 = -0.54(\pm 0.005)$  in layer 1 is even negative. These evidences show that the correlation between  $\|(HW)_{[i]}\|$  and  $\|P^{[i]}\|$  is pretty unstable and might be even negative, which violates the assumption that  $\|(HW)_{[i]}\| \propto \|P^{[i]}\|$ . Similar patterns are also observed on the other datasets. More regression results and experimental details are presented in Appendix A.4.

## 4.2 Proposed Sampling Probabilities

As analyzed above, the sampling probabilities in LADIES are sub-optimal due to the failure of their assumption. To address this issue, we instead admit that we have no prior knowledge of  $\mathbf{HW}$ , and tend to assume a uniform distribution of  $\|(HW)_{[i]}\|$ 's. With this belief we propose the following sampling probabilities:

$$p_i \propto \|QP^{[i]}\|, \quad \forall i \in [n]. \quad (5)$$

Compared to the sampling probabilities of LADIES in Equation (2), our proposed sampling probabilities  $p_i$ 's are more conservative. From a matrix approximation perspective, we rewrite the target matrix product as  $QPIHW$ , and only aim to approximate the known part  $QPI$ . It turns out that assuming the uniform distribution of the norms of rows in  $\mathbf{HW}$  can help improve both the variance of the matrix approximation and the prediction accuracy of GCNs. We empirically justify our sampling probabilities in the next section and Section 6.

In addition to the empirical results, we compare the sampling variance of our probabilities with LADIES in Lemma C.1. We remark that the sampling variance depends on the underlying distribution of the row norms of  $\mathbf{HW}$ , and therefore no sampling probability can always have a smaller variance. Specifically, we find that the common long-tail distribution of  $\mathbf{HW}$  can justify the strengths of our new probabilities. More discussion and visualization on the distribution of  $\mathbf{HW}$  are provided in Appendix C.

### 4.3 Matrix Approximation Results

To further justify our proposed sampling probability, we consider the following 1-layer matrix approximation error, which evaluates the propagation approximation to the embedding aggregation of full-batch.

$$\|\tilde{\mathbf{Z}}_{batch}^{(1)} - \tilde{\mathbf{Z}}_{sampling}^{(1)}\|_F = \|\mathbf{Q}_{batch} \mathbf{P} \mathbf{H}^{(0)} \mathbf{W}^{(0)} - \mathbf{Q}_{batch} \mathbf{P} \mathbf{S} \mathbf{H}^{(0)} \mathbf{W}^{(0)}\|_F,$$

where  $\tilde{\mathbf{Z}}_{batch}^{(1)}$  and  $\tilde{\mathbf{Z}}_{sampling}^{(1)}$  are the embedding at the bottom layer for the whole batch (using all available neighbors without sampling) and for a certain sampling method;  $\mathbf{S}$  is the sampling matrix;  $\mathbf{Q}_{batch}$ 's 0, 1 diagonal entries indicate if a node is in the batch;  $\|\cdot\|_F$  denotes the Frobenius norm of a matrix. The experiments are repeated 200 times, in which we regenerate the batch nodes (shared by all sampling methods) and the sampling matrix for each method. The batch size is fixed as 512 and the numbers of sampled neighbors are 256, 512, 768, 1024, 2536, and 2048.  $\mathbf{W}^{(0)}$  is fixed and inherited from the trained model reported in Section 6.

In Figure 1, the result of our proposed sampling probabilities (denoted as ‘‘LAIDES+flat’’, blue solid line) is consistently better than that of the original LADIES method (black dashed line) and of FastGCN (black solid line) on every dataset. This supports the new sampling probability in Equation (5). We will discuss the debiasing methods in this figure in Section 5.

## 5 Debaised Sampling

We first make the clarification that previous layer-wise sampling strategies (Chen et al., 2018b; Zou et al., 2019) assume the neighbor nodes are sampled with replacement, and are proved to be unbiased approximations of GCN embedding. However, in their practical implementations, sampling is always performed without replacement, which induces biases since the estimators are still constructed based on the expression for sampling with replacement. We illustrate the biases in Figure 1, where the matrix approximation errors on ogbn-arxiv and ogbn-mag datasets (sparse graphs with few average degrees) are U-shape for the LADIES algorithm. The curve indicates that the errors even increase with the number of sub-samples, and the approximation performance is heavily deteriorated by the biases.

In the following subsections, we dive into the implementation of FastGCN and LADIES, reveal the origin of the biases, propose a new debiasing method for sampling without replacement, and study the statistical properties of the debaised estimators.

**Remark.** We insist sampling without replacement because it helps reduce the variance of the estimator. Current node-wise sampling GCNs also sample ‘‘without replacement’’—they apply simple random sampling (SRS, sampling with all-equal probabilities), which is guaranteed to shrink the variance by a finite population correction (FPC) factor  $\frac{n-s}{n-1}$  (Lohr, 2019, Section 2.3)<sup>1</sup>.

### 5.1 Weighted Random Sampling (WRS)

The implementation of layer-wise importance sampling (without replacement) follows a sequential procedure named as weighted random sampling (WRS) (Efraimidis & Spirakis, 2006, Algorithm D). Given a set  $V = [n]$  representing the indices of  $n$  items  $\{\mathbf{X}_i\}_{i=1}^n$ <sup>2</sup> and the associated sampling probabilities  $\{p_i\}_{i=1}^n$ , we want to sample  $s$  samples and denote the sampled indices as  $I_k$  for  $k = 1, 2, \dots, s$ .

The implementation of previous layer-wise sampling methods uses the following estimator to approximate  $\sum_{i=1}^n \mathbf{X}_i$  (adapted to the notations in this subsection)

$$\frac{1}{s} \sum_{k=1}^s \mathbf{X}_{I_k} / p_{I_k}, \tag{6}$$

which is biased when sampling without replacement.

<sup>1</sup> $s$  and  $n$  denote the sample size and the population size.

<sup>2</sup>In layer-wise sampling,  $\mathbf{X}_i$  represents  $\mathbf{B}^{[i]} \mathbf{C}_{[i]}^T$ , where for brevity  $\mathbf{QP} (HW)$  is denoted as  $\mathbf{B} (C)$  throughout the analysis.

Equation (6) can be viewed a weighted average of  $X_{I_k}$ 's. We aim to preserve the linear form  $\mathbf{Y}_s := \sum_{k=1}^s \beta_k \mathbf{X}_{I_k}$  in debiasing, and develop new coefficients  $\beta_k$  for each  $X_{I_k}$  to make  $Y_s$  unbiased. The debiasing algorithm is presented in Section 5.3.

## 5.2 Analysis of Bias

To analyze the bias in Equation (6), we further introduce the following notations. Specifically, aside from the set  $S_k$  of  $k$  previously sampled indices ( $0 \leq k \leq s-1, S_0 := \emptyset$ ), the  $(k+1)$ -th random index  $I_{k+1}$  is sampled from the set  $V - S_k$  of the rest  $n - k$  indices with probabilities

$$\begin{aligned} p_i^{(0)} &:= p_i, & \forall i \in V = [n], \\ p_i^{(k)} &:= \frac{p_i}{\sum_{j \in V - S_k} p_j}, & \forall k \in [s-1], i \in V - S_k. \end{aligned}$$

With the notations introduced, we are now able to analyze the effect of directly using Equation (6) while the WRS algorithm is performed. The expectation of a certain summand  $\mathbf{X}_{I_{k+1}}/p_{I_{k+1}}$  will be

$$\mathbb{E} \frac{\mathbf{X}_{I_{k+1}}}{p_{I_{k+1}}} = \mathbb{E} \left[ \mathbb{E} \left[ \frac{\mathbf{X}_{I_{k+1}} p_{I_{k+1}}^{(k)}}{p_{I_{k+1}}^{(k)} p_{I_{k+1}}} \mid \mathcal{F}_k \right] \right] = \mathbb{E} \left[ \frac{1}{\sum_{i \in V - S_k} p_i} \sum_{i \in V - S_k} \mathbf{X}_i \right], \quad (7)$$

where  $\mathcal{F}_k$  is the  $\sigma$ -algebra generated by the random indices inside the corresponding set  $S_k, \forall k = 0, 1, \dots, s-1$ , and the second equation holds because  $\frac{p_{I_{k+1}}^{(k)}}{p_{I_{k+1}}} = \frac{1}{\sum_{i \in V - S_k} p_i}$  is  $\mathcal{F}_k$ -measurable. The expectation is in general unequal to the target  $\sum_{i=1}^n \mathbf{X}_i$  for  $k > 0$ , except for some extreme conditions such as all-equal  $p_i$ 's. The bias in each summand (except for the first term with  $k = 0$ ) accumulates and results in the ultimate bias in the given estimation.

## 5.3 Debiasing Algorithm

We start with a review of existing works. The bias induced by the sequential WRS algorithm has been extensively analyzed by many studies, especially the ones on stochastic gradient estimators (Liang et al., 2018; Liu et al., 2019; Kool et al., 2019). Given a sequence of random indices sampled through WRS, there are two common genres to assign coefficients to summands in Equation (6). Both of the two methods relate to the *stochastic sum-and-sample* estimator (Liang et al., 2018; Liu et al., 2019), which can be derived from Equation (7). Using the fact  $\mathbb{E} \frac{\mathbf{X}_{I_{k+1}}}{p_{I_{k+1}}} \sum_{i \in V - S_k} p_i = \mathbb{E} [\sum_{i \in V - S_k} \mathbf{X}_i]$ , a stochastic sum-and-sample estimator of  $\sum_{i=1}^n \mathbf{X}_i$  can be immediately constructed as

$$\mathbf{\Pi}_{k+1} = \sum_{j \in S_k} \mathbf{X}_j + \frac{\mathbf{X}_{I_{k+1}}}{p_{I_{k+1}}^{(k)}}, \forall k = 0, 1, \dots, s-1. \quad (8)$$

(The proof of unbiasedness is brief and provided by Kool et al. (2019, Appendix C.1).) To minimize the variance, Liang et al. (2018); Liu et al. (2019) develop the first genre to focus on the last estimator  $\mathbf{\Pi}_s$  and propose methods to pick the initial  $s-1$  random indices. Kool et al. (2019, Theorem 4) turn to the second genre which utilize Rao-Blackwellization (Casella & Robert, 1996) of  $\mathbf{\Pi}_s$ .

In fast training for GCN, both of the two genres are somewhat inefficient from a practitioner's perspective. The first genre works well when  $\sum_{i \in S_{s-1}} p_i$  is close to 1, otherwise the last term in  $\mathbf{\Pi}_s, \frac{\mathbf{X}_{I_{k+1}}}{p_{I_{k+1}}^{(k)}}$ , will bring in large variance and reduce the sample efficiency; for the second genre, the time cost to perform Rao-Blackwellization (Kool et al., 2019) is extremely high ( $\mathcal{O}(2^s)$  even with approximation by numerical integration) and conflicts with the purpose of fast training. To overcome the issues of the two existing genres, we propose an iterative method to fully utilize each estimator  $\mathbf{\Pi}_{k+1}$  with acceptable runtime to decide the coefficients for each term in Equation (6).

---

**Algorithm 1:** Iterative updates of coefficients to construct the ultimate debiased estimator  $\mathbf{Y}_s$

---

**Input:** probabilities  $\{p_i\}_{i=1}^n$ , random indices  $\{I_{k+1}\}_{k=0}^{s-1}$  generated by WRS with  $\{p_i\}_{i=1}^n$

**Output:** a length  $s$  coefficient vector  $\beta$

Initialize  $\beta = \mathbf{0} \in \mathbb{R}^s$ ,  $p_S = 0$  (sum of probabilities);

**for**  $k \leftarrow 0$  **to**  $s - 1$  **do**

$$\alpha_{k+1} = \frac{n}{(n-k)(k+1)};$$

$$\beta_{[k+1]} = \alpha_{k+1}(1 - p_S)/p_{I_{k+1}};$$

**for**  $j \leftarrow 0$  **to**  $k - 1$  **do**

$$\quad | \quad \beta_{[j+1]} = (1 - \alpha_{k+1})\beta_{[j+1]} + \alpha_{k+1};$$

**end**

$$p_S = p_S + p_{I_{k+1}};$$

**end**

return  $\beta$ ;

---

Denote our final estimator with  $s$  samples as  $\mathbf{Y}_s$ . Our Algorithm 1 returns the coefficients  $\beta_k$ 's in the estimator  $\mathbf{Y}_s = \sum_{k=1}^s \beta_k \mathbf{X}_{I_k}$  (??). The idea is perform recursive estimation  $\mathbf{Y}_1, \mathbf{Y}_2, \dots$  until  $\mathbf{Y}_s$  and thus update  $\beta$  accordingly.

To be more specific, we recursively perform the weighted averaging below:

$$\mathbf{Y}_0 := \mathbf{0}, \quad \mathbf{Y}_{k+1} := (1 - \alpha_{k+1})\mathbf{Y}_k + \alpha_{k+1}\mathbf{\Pi}_{k+1},$$

$\forall k = 0, 1, \dots, s - 1$ , where  $\alpha_{k+1}$  is a constant depends on  $k$ . When  $\alpha_1 = 1$ ,  $\mathbf{Y}_1 = \mathbf{\Pi}_1 = \mathbf{X}_{I_1}/p_{I_1}$  is unbiased and the unbiasedness of  $\mathbf{Y}_s$  can be obtained by induction as each  $\mathbf{\Pi}_{k+1}$  is unbiased as well. There can be alternative choices of  $\alpha_{k+1}$ 's. For example, *the stochastic sum-and-sample estimator* (8) (Liang et al., 2018; Liu et al., 2019) will produce different  $\alpha_{k+1}$ 's from ours. In our algorithm, we intentionally specify  $\alpha_{k+1} = \frac{n}{(n-k)(k+1)}$ , motivated by the preference that if all  $p_i$ 's are  $1/n$ , the output coefficients of the algorithm will be all  $1/s$ , the same as the ones in an SRS setting.

The time complexity of Algorithm 1 is  $\mathcal{O}(s^2)$ , as in  $k$ -th iteration we update the coefficients for the first  $k$  random indices sampled. The time complexity is comparable to the one of embedding aggregation in layer-wise training, as shown in Appendix B. We further conduct sampling experiments on the CPU to compare the debiasing cost to the sampling cost. Both batch size and sampling size are fixed as 512 nodes. The results in Table 3 confirm that the debiasing algorithm does not add too much burden to the original sampling procedure. We remark that the inefficiency of node-wise sampling comes from the overhead cost in the sparse matrix. We also note that FastGCN, LADIES, and our methods can prepare the sampled Laplacian matrices on CPU separately from the training on the GPU. This does not hold for VR-GCN, which requires up-to-date embedding information. More experimental details, including additional results with more sampled nodes on all datasets are deferred to Appendix A.3.

Table 3: Average sampling time (in milliseconds) per batch for layer-wise methods and vanilla node-wise method.

	arxiv	proteins	products
Node-wise	585.2 $\pm$ 3.6	830.9 $\pm$ 5.3	2795.4 $\pm$ 4.7
FastGCN	4.2 $\pm$ 0.1	11.1 $\pm$ 1	54.8 $\pm$ 0.7
LADIES	8.3 $\pm$ 0.1	11.2 $\pm$ 0.3	83.4 $\pm$ 1.3
w/ flat	7.8 $\pm$ 0.1	10 $\pm$ 0.2	80.3 $\pm$ 0.4
w/ debias	11.7 $\pm$ 0.2	13.6 $\pm$ 0.2	83.7 $\pm$ 0.8
w/ flat+debias	11.7 $\pm$ 0.5	12.6 $\pm$ 0.2	83.5 $\pm$ 0.6

## 5.4 Effects of Debiasing

Again, we evaluate the performance of the debiasing algorithm by matrix approximation error (see Section 4.3). Based on the results in Figure 1, our proposed debiasing method can significantly improve the single-

step matrix approximation error on all datasets. In particular, by introducing the biasing algorithm, the U-shape curve no longer exists, which means the error consistently decreases when increasing the sample size. If the new sampling probabilities have already been applied (LADIES + flat in Figure 1), additional debiasing algorithm (LADIES + flat + debiased) only makes marginal improvement on sparse graphs (ogbn-arxiv and ogbn-mag). This implies that the effect of debiasing and new sampling probabilities may have overlaps. We provide the following conjectures for this phenomenon. First, since the bias is introduced by sampling without replacement, it is significant only when the proportion of sampled nodes over all neighbors large enough. When increasing the sample size, it is obvious that sparse graphs will reach a large “sampling proportion” earlier than dense graphs. Second, our proposed sampling probabilities have a flatter distribution than LADIES. So the bias of “LADIES + flat” is already smaller than “LADIES”, since the sampling probabilities are closer to the uniform distribution.

We note that the debiasing algorithm can also accelerate the convergence and increase the model prediction accuracy. The evidence is provided in Section 6. and as the biases accumulate, the effect of the debiasing algorithm emerges.

## 5.5 Analysis of variance

In sampling without replacement, the selected samples are no longer independent, and therefore the classical analysis in previous works (c.f. Lemma C.2 in Appendix C) cannot be applied to the variance of WRS-based estimators. To quantify the variance under the WRS setting, we leverage a common technique in experimental design—viewing  $\{\beta_i^{(k)}\}_{i=1}^n, \forall k \in [s]$  as random variables to analyze, which denote the coefficients assigned to  $\mathbf{X}_i$ ’s when the  $k$ -th sample is drawn (if  $i \notin S_k$ ,  $\beta_i^{(k)} := 0$ ). This technique can derive the same result as in the previous random indices ( $I_k$ ’s) setting, while allow a finer analysis of the variance. We rewrite the variance in Equation (4) as <sup>3</sup>

$$\mathbb{E} \|\mathbf{BSC} - \mathbf{BC}\|_F^2 = \sum_{j,k} \text{Var} \left( \sum_{i=1}^n \beta_i^{(s)} \mathbf{B}_j^{[i]} \mathbf{C}_{[i],k} \right).$$

The above variance is determined by the covariance matrix  $\text{Cov}(\boldsymbol{\beta})$ , whose  $(i, j)$ -th element is  $\text{Cov}(\beta_i^{(s)}, \beta_j^{(s)})$ . We provide the following proposition:

**Theorem 1.** *For all  $k \in [s]$ , let  $p_{S_k}$  be the probability of having  $S_k$  as the first  $k$  samples,  $\bar{q}_i^{(k)}$  be the probability of index  $i$  not in the  $k$  samples, and  $\bar{q}_{i,j}^{(k)}$  be the probability of both index  $i, j$  not in the  $k$  samples. Define  $r_i^{(k)} := \sum_{S_k \not\ni i} p_{S_k} (1 - \sum_{j \in S_k} p_j)$ , where  $\sum_{S_k \not\ni i}$  iterates over all  $S_k$  that does not contain  $i$ . Then  $\text{Var}(\beta_i^{(k+1)}) \geq 0$  and  $\text{Cov}(\beta_i^{(k+1)}, \beta_j^{(k+1)}) \leq 0$  are recursively given as:*

$$(1 - \alpha_{k+1})^2 \text{Var}(\beta_i^{(k)}) + \left( \frac{r_i^{(k)}}{p_i} - \alpha_{k+1}^2 \bar{q}_i^{(k)} \right), \quad (9)$$

$$(1 - \alpha_{k+1})^2 \text{Cov}(\beta_i^{(k)}, \beta_j^{(k)}) - \alpha_{k+1}^2 \bar{q}_{i,j}^{(k)}. \quad (10)$$

Furthermore, there exists a sequence  $\{\alpha_k\}_{k=1}^s$  only depending on  $k, n$  such that for all  $i, j$ ,  $\text{Var}(\beta_i^{(k)}) \leq \frac{1}{k} (\frac{1}{p_i} - 1)$ ,  $|\text{Cov}(\beta_i^{(k)}, \beta_j^{(k)})| \leq \frac{1}{k}, \forall k \in [s]$ .

Proof and discussions are collected in Appendix C.4. We remark that due to the fixed weights  $\alpha_k = 1$  in the stochastic sum-and-sample estimator (8), its (co)variance is usually larger than ours, especially when  $k \ll n$  (recall for SRS,  $\bar{q}_{i,j}^{(k)} = \binom{n-2}{k} / \binom{n}{k}$ ).

## 6 Experiments

In this section, we empirically evaluate the performance of each method on five node prediction datasets: Reddit, ogbn-arxiv, ogbn-proteins, ogbn-mag, ogbn-products (c.f. Table 1). We denote “LADIES+flat”,

<sup>3</sup>We let  $\mathbf{B}$  ( $\mathbf{C}$ ) have  $n$  columns (rows), and the  $j(k)$ -th element in the  $i$ -th column (row) is denoted as  $\mathbf{B}_j^{[i]}$  ( $\mathbf{C}_{[i],k}$ ).

Table 4: Prediction accuracy on benchmarks. The best accuracy among layer-wise sampling methods and all methods are both highlighted in boldface. The accuracy is in percentage (%). The averaged training time for one epoch is in milliseconds.

	Accuracy					Epoch avg. train. time	
	Reddit	ogbn-arxiv	ogbn-mag	ogbn-protein	ogbn-product	ogbn-arxiv	ogbn-product
Full-batch	93.81±0.18	66.39±0.25	29.60±0.27	65.71±0.11	68.33±0.16	65.2 ± 3.97	703 ± 77.8
Node-wise (2)	92.13±0.27	64.51±0.30	29.05±0.45	65.76±0.18	68.71±0.07	22.0 ± 3.64	8.34 ± 1.21
VR-GCN (2)	<b>94.62±0.04</b>	<b>67.49±0.25</b>	28.99±0.40	67.45±0.02	<b>70.90±0.28</b>	86.8 ± 6.09	88.5 ± 2.51
GraphSAINT	89.47±0.83	60.58±0.62	24.77±0.88	66.33±0.07	62.77±1.04	23.1 ± 3.26	8.26 ± 1.11
FastGCN	44.46±2.30	25.44±0.82	7.13±0.48	52.44±1.88	26.98±0.42	24.1 ± 5.12	7.43 ± 1.04
LADIES	73.86±0.17	60.95±0.31	24.79±0.48	68.28±0.05	52.97±1.11	19.3 ± 3.25	10.3 ± 1.24
w/ flat	90.04±0.11	62.76±0.26	27.30±0.27	68.26±0.06	62.64±0.10	16.0 ± 2.37	8.03 ± 1.07
w/ debias	86.73±0.36	61.55±0.40	25.74±0.80	68.87±0.09	55.92±0.92	19.1 ± 3.45	8.44 ± 1.09
w/ flat & debias	89.34±0.40	61.90±0.43	27.41±0.28	67.64±0.15	62.57±0.22	14.6 ± 2.59	8.11 ± 1.09
FastGCN (2)	60.31±0.70	30.23±1.10	5.85±0.57	58.80±1.06	31.58±0.70	24.9 ± 5.09	8.34 ± 1.11
LADIES (2)	88.34±0.11	64.01±0.39	28.59±0.39	68.17±0.10	65.24±0.40	21.0 ± 4.00	11.2 ± 1.35
w/ flat	93.64±0.19	<b>66.56±1.84</b>	29.58±0.19	68.10±0.07	68.47±0.25	23.1 ± 4.04	13.1 ± 1.52
w/ debias	92.75±0.22	65.93±0.27	<b>30.08±0.28</b>	<b>69.14±0.15</b>	67.18±0.24	14.0 ± 1.94	8.54 ± 1.09
w/ flat & debias	<b>93.59±0.09</b>	66.22±0.10	29.88±0.34	67.75±0.11	<b>68.49±0.06</b>	21.0 ± 3.60	8.50 ± 1.15

“LADIES+debiased”, and “LADIES+flat+debiased” respectively as the variants of LADIES with the improvements from Section 4, Section 5, and from both. We compare our methods to the original GCN with mini-batch stochastic training (denoted by full-batch), two layer-wise sampling methods: FastGCN and LADIES. Apart from that, we also implement several other fast GCN training methods, including GraphSAGE (Hamilton et al., 2017) (vanilla node-wise sampling while keep using the GCN architecture), VR-GCN (Chen et al., 2018a), and subgraph sampling method GraphSAINT (Zeng et al., 2019).

In the model training, we use a 2-layer GCN for each task with an ADAM optimizer of a learning rate 0.001. (Due to limited computational resources, we have to use the shallow GCN since the full-batch method and node-wise sampling methods require much more GPU memory even when  $L = 3$ .) The number of hidden variables is 256 and the batch size is 512. For layer-wise sampling methods, we consider two settings of node sampling number: 1) fixed as equal to the batch size (512); 2) an “increasing” setting (denoted with (2)) that twice nodes will be sampled in the next layer. For the node-wise sampling methods (GraphSAGE, VR-GCN), the number of neighbors per node is 2 (denoted with (2)). For the subgraph sampling method GraphSAINT (Zeng et al., 2019), the subgraph size is by default equal to the batch size. The experiment results are reported in Table 4, in the form of “mean(±std.)”, computed based on 5 runs. More details of the settings are deferred to Appendix A.1.

## 6.1 Model Convergence Trajectory

We first compare the convergence rates of layer-wise methods. Here, we exclude FastGCN due to its poor performance. The convergence curve on ogbn-proteins and ogbn-products are shown in Figure 3. The results of all methods (including node-wise and subgraph) on every dataset are deferred to Figure 4 in Appendix A.2.

In Figure 3 (and Figure 4 in the appendix), we observe our proposed improvements (LADIES + flat, LADIES + debias, LADIES + flat + debias) show faster convergence rate than LADIES (the solid blue curve). This means both the new sampling probabilities (“flat”) and the debiasing algorithm can accelerate the training. We also note that they may have overlapped effects. Regarding the convergence, we also observe that the effect of debiasing is not as significant as choosing a proper sampling scheme on some datasets, such as ogbn-products dataset. This can be possibly explained by our analysis in Section 5.4.

## 6.2 Prediction Accuracy

The prediction accuracy on the test sets of different datasets is reported in Table 4. We observe the performance of our methods, which combines the new sampling probabilities and the debiasing algorithm, are comparable to the full-batch training (no further sampling), showing consistent improvement over existing



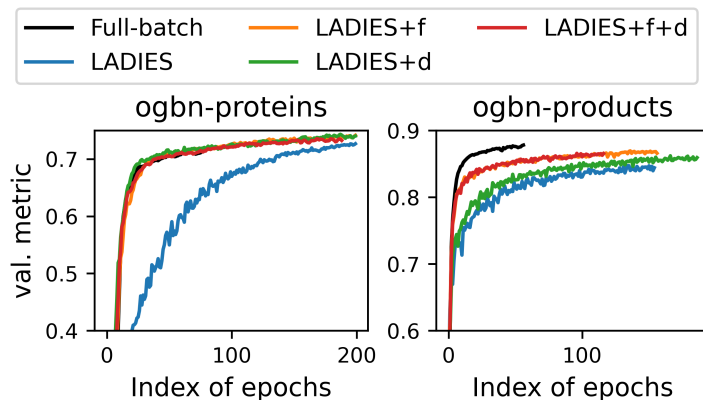


Figure 3: Curves of accuracy on the validation sets in each epoch. “f” and “d” refer to the “flat” sampling probability and “debiasing” respectively. The layer-wise sampling methods follow the “increasing” setting (denoted with the suffix (2) in Table 4).

layer-wise sampling methods, FastGCN and LADIES. On most benchmarks, the prediction performance of our methods is better than the vanilla node-wise sampling method (GraphSAGE) and GraphSAINT. In addition, the experiments further verify the previous observation that the two remedies we apply have the overlapping effect, which is implied in Figure 1 and Figure 3 that (when sub-sample size is small) the improvement of “LADIES+flat+debiased” over its ablation method “LADIES+flat” may be insignificant.

As for the training time (see Table 4), our proposed methods have similar training time with LADIES since these layer-wise sampling strategies have the same propagation scheme. We note that though VR-GCN achieves the best accuracy on three benchmarks, it suffers from a much heavier computational cost than the layer-wise methods, at the expense of involving historical embedding. In particular, its training time is even comparable to the full-batch method on ogbn-arxiv data.

We close this section with a remark on the seemingly strange phenomenon that some efficient GCNs have a higher prediction accuracy than full-batch GCN on several datasets. We speculate the reason is that a good approximation can recover the principal components in the original embedding matrix, and also restrain the noise via the sparse / low-rank structure. There is a similar observation (Sanyal et al., 2018) in Convolutional Neural Networks (CNN) as well, that applying a low-rank regularizer, such as SVD, to the representation of the intermediate layers can improve the prediction accuracy of CNN models.

## 7 Conclusion and Discussion

We carefully analyze the existing layer-wise sampling strategies and propose two improvements. We first show that a conservative choice of sampling probabilities outperforms the existing ones, whose assumption is usually too strong in practice. We further propose a recursive debiasing algorithm for the layer-wise importance sampling, and provide statistical analysis.

One possible extension of our work is to apply the other techniques in approximate matrix multiplication to the fast training in GCN. Some possible choices include a very sparse random projection (Li et al., 2006), sparse oblivious subspace embedding (Cohen, 2016), and accumulative sketching (Chen & Yang, 2021). Another direction of future research is the extension of our method to broader classes of graph neural networks, in a way similar to the work by Liu et al. (2020).

---

## References

- Michael M Bronstein, Joan Bruna, Yann LeCun, Arthur Szlam, and Pierre Vandergheynst. Geometric deep learning: going beyond euclidean data. *IEEE Signal Processing Magazine*, 34(4):18–42, 2017.
- Joan Bruna, Wojciech Zaremba, Arthur Szlam, and Yann LeCun. Spectral networks and deep locally connected networks on graphs. In *2nd International Conference on Learning Representations, ICLR 2014*, 2014.
- George Casella and Christian P Robert. Rao-blackwellisation of sampling schemes. *Biometrika*, 83(1):81–94, 1996.
- Jianfei Chen, Jun Zhu, and Le Song. Stochastic training of graph convolutional networks with variance reduction. In *International Conference on Machine Learning*, pp. 942–950. PMLR, 2018a.
- Jie Chen, Tengfei Ma, and Cao Xiao. Fastgcn: Fast learning with graph convolutional networks via importance sampling. In *International Conference on Learning Representations*, 2018b.
- Yifan Chen and Yun Yang. Accumulations of projections—a unified framework for random sketches in kernel ridge regression. *arXiv preprint arXiv:2103.04031*, 2021.
- Wei-Lin Chiang, Xuanqing Liu, Si Si, Yang Li, Samy Bengio, and Cho-Jui Hsieh. Cluster-gcn: An efficient algorithm for training deep and large graph convolutional networks. In *Proceedings of the 25th ACM SIGKDD International Conference on Knowledge Discovery & Data Mining*, pp. 257–266, 2019.
- Michael B Cohen. Nearly tight oblivious subspace embeddings by trace inequalities. In *Proceedings of the twenty-seventh annual ACM-SIAM symposium on Discrete algorithms*, pp. 278–287. SIAM, 2016.
- Weilin Cong, Rana Forsati, Mahmut Kandemir, and Mehrdad Mahdavi. Minimal variance sampling with provable guarantees for fast training of graph neural networks. In *Proceedings of the 26th ACM SIGKDD International Conference on Knowledge Discovery & Data Mining*, pp. 1393–1403, 2020.
- Zhiyong Cui, Kristian Henrickson, Ruimin Ke, and Yin Hai Wang. Traffic graph convolutional recurrent neural network: A deep learning framework for network-scale traffic learning and forecasting. *IEEE Transactions on Intelligent Transportation Systems*, 21(11):4883–4894, 2019.
- Michaël Defferrard, Xavier Bresson, and Pierre Vandergheynst. Convolutional neural networks on graphs with fast localized spectral filtering. In *NIPS*, 2016.
- Petros Drineas, Ravi Kannan, and Michael W Mahoney. Fast monte carlo algorithms for matrices i: Approximating matrix multiplication. *SIAM Journal on Computing*, 36(1):132–157, 2006.
- Pavlos S Efrimidis and Paul G Spirakis. Weighted random sampling with a reservoir. *Information Processing Letters*, 97(5):181–185, 2006.
- William L Hamilton, Zhitaoying, and Jure Leskovec. Inductive representation learning on large graphs. In *NIPS*, 2017.
- Weihua Hu, Matthias Fey, Marinka Zitnik, Yuxiao Dong, Hongyu Ren, Bowen Liu, Michele Catasta, and Jure Leskovec. Open graph benchmark: Datasets for machine learning on graphs. *Neural Information Processing Systems (NeurIPS)*, 2020.
- Wenbing Huang, Tong Zhang, Yu Rong, and Junzhou Huang. Adaptive sampling towards fast graph representation learning. *Advances in Neural Information Processing Systems*, 31:4558–4567, 2018.
- Thomas N. Kipf and Max Welling. Semi-supervised classification with graph convolutional networks. In *5th International Conference on Learning Representations, ICLR 2017, Toulon, France, April 24-26, 2017, Conference Track Proceedings*. OpenReview.net, 2017. URL <https://openreview.net/forum?id=SJU4ayYgl>.

- 
- Wouter Kool, Herke van Hoof, and Max Welling. Estimating gradients for discrete random variables by sampling without replacement. In *International Conference on Learning Representations*, 2019.
- Ping Li, Trevor J Hastie, and Kenneth W Church. Very sparse random projections. In *Proceedings of the 12th ACM SIGKDD international conference on Knowledge discovery and data mining*, pp. 287–296, 2006.
- Chen Liang, Mohammad Norouzi, Jonathan Berant, Quoc Le, and Ni Lao. Memory augmented policy optimization for program synthesis and semantic parsing. In *Proceedings of the 32nd International Conference on Neural Information Processing Systems*, pp. 10015–10027, 2018.
- Runjing Liu, Jeffrey Regier, Nilesh Tripuraneni, Michael Jordan, and Jon McAuliffe. Rao-blackwellized stochastic gradients for discrete distributions. In *International Conference on Machine Learning*, pp. 4023–4031. PMLR, 2019.
- Ziqi Liu, Zhengwei Wu, Zhiqiang Zhang, Jun Zhou, Shuang Yang, Le Song, and Yuan Qi. Bandit samplers for training graph neural networks. *Advances in Neural Information Processing Systems*, 33, 2020.
- Sharon L Lohr. *Sampling: design and analysis*. Chapman and Hall/CRC, 2019.
- Afshin Rahimi, Trevor Cohn, and Timothy Baldwin. Semi-supervised user geolocation via graph convolutional networks. In Iryna Gurevych and Yusuke Miyao (eds.), *Proceedings of the 56th Annual Meeting of the Association for Computational Linguistics, ACL 2018, Melbourne, Australia, July 15-20, 2018, Volume 1: Long Papers*, pp. 2009–2019. Association for Computational Linguistics, 2018. doi: 10.18653/v1/P18-1187. URL <https://www.aclweb.org/anthology/P18-1187/>.
- Amartya Sanyal, Varun Kanade, Philip HS Torr, and Puneet K Dokania. Robustness via deep low-rank representations. *arXiv preprint arXiv:1804.07090*, 2018.
- Michael Schlichtkrull, Thomas N Kipf, Peter Bloem, Rianne Van Den Berg, Ivan Titov, and Max Welling. Modeling relational data with graph convolutional networks. In *European semantic web conference*, pp. 593–607. Springer, 2018.
- Zonghan Wu, Shirui Pan, Fengwen Chen, Guodong Long, Chengqi Zhang, and S Yu Philip. A comprehensive survey on graph neural networks. *IEEE transactions on neural networks and learning systems*, 2020.
- Rex Ying, Ruining He, Kaifeng Chen, Pong Eksombatchai, William L Hamilton, and Jure Leskovec. Graph convolutional neural networks for web-scale recommender systems. In *Proceedings of the 24th ACM SIGKDD International Conference on Knowledge Discovery & Data Mining*, pp. 974–983, 2018.
- Hanqing Zeng, Hongkuan Zhou, Ajitesh Srivastava, Rajgopal Kannan, and Viktor Prasanna. Graphsaint: Graph sampling based inductive learning method. In *International Conference on Learning Representations*, 2019.
- Difan Zou, Ziniu Hu, Yewen Wang, Song Jiang, Yizhou Sun, and Quanquan Gu. Layer-dependent importance sampling for training deep and large graph convolutional networks. *Advances in neural information processing systems*, 2019.

---

## A Additional Experiment Details

### A.1 Additional Details on Experimental Setups

In this section, we describe the additional details of experiment setups for Section 6. All the models are implemented by Pytorch. We use one Tesla V100 SXM2 16GB GPU with 10 CPU threads to train the models in Section 6. Our implementation of Full-batch method, FastGCN, and LADIES are adapted from the codes by Zou et al. (2019); the implementation of vanilla node-wise sampling, VR-GCN, GraphSAINT is adapted from the codes by Cong et al. (2020). For the vanilla node-wise sampling method, there are several variants of structures Ying et al. (2018) while we fix the model structure as GCN in our experiments for fair comparison. We use ELU as the activation function in the convolutional layer for all the models:  $\text{ELU}(x) = x$  for  $x > 0$ ,  $\text{ELU}(x) = \exp(x) - 1$  for  $x \leq 0$ . We choose dropout rate as 0.2, which means 20 percents of units are randomly dropped during the training. Validation and testing are performed with Full-batch inference (using all possible neighbors) on validation and testing nodes. Note that some existing Pytorch implementations of GCNs involve several ad-hoc tricks, such as row-normalizing sampled Laplacian matrix. For the accuracy evaluation experiments in Section 6, we stop training when the validation F1 score does not increase for 200 batches. For a fair comparison, we remove certain tricks in our experiments, such as normalization of each rows in the sampled Laplacian matrix in layer-wise sampling. Such a trick may help in the practice but it might not be compatible with some other methods and is out of the focus of our study. We use the metrics in Table 1 to evaluate the accuracy of each method. Concretely, Reddit is a multi-class classification task and we use the Micro-F1 score with function “sklearn.metrics.f1\_score”. For OGB data, we use the built-in evaluator function in module `ogb` by Hu et al. (2020).

### A.2 Additional Results on Model Convergence

Figure 4 is a supplementary to Figure 3. We present the convergence curve of all methods on every benchmark. The setting of each model is the same as in Figure 3.

### A.3 Additional Results on Sampling Time and Training Time

We compare the sampling time per batch for 1-layer GCN with layer-wise sampling methods (FastGCN, LADIES, and our proposed methods) and GraphSAGE by experiments on CPU. The time is presented in milliseconds. The batch size is 512, and the number of sampled nodes is 512 or 1024. The average sampling time (followed by standard deviation) over 200 batches is presented in Table 3. We note that the sampling time may involve some overhead costs. For example, the input Laplacian matrix is Scipy-sparse-matrix on the CPU, while in sampling, it is converted to a PyTorch-sparse-matrix.

By Table 3, we conclude that the cost of debiasing algorithm is acceptable. Moreover, since the debiasing only depends on the number of nodes sampled, its time cost will be dwarfed by sampling on very large graphs. For example, sampling 512 nodes, the average batch sampling time for “LADIES”, “LADIES + debiased”, “LADIES + flat + debiased”, are  $8.3 \pm 0.1$ ,  $11.7 \pm 0.2$ ,  $11.7 \pm 0.5$  respectively on ogbn-arxiv while  $83.4 \pm 1.3$  and  $83.7 \pm 0.8$  and  $83.5 \pm 0.6$  respectively on ogbn-products data. As we mentioned in Section 5.3, the node-wise sampling takes a significantly longer time because individually sampling from each row in the re-normalized Laplacian matrix (stored as a sparse matrix in implementation) leads to a large overhead cost.

We present the training time (per batch) of 2-layer and 3-layer GCNs in Tables 6 and Table 7 respectively. The time is presented in millisecond and averaged over 110 batches, where we discard the first 20 and the last 20 out of 150 total batches to disregard potential warm-up time for GPU. The other settings are kept the same as our experiments of accuracy evaluation in Table 4. We note that the timing on GPU is sensitive to the hardware and has a relatively large standard deviation.

As presented in Tables 6 and 7, our proposed methods have similar training time with LADIES due to the same propagation scheme of GCN with layer-wise sampling strategy. The VR-GCN generally shows superiority in prediction accuracy (see Table 4). However, it also takes a significantly longer time in training since its propagation involves using and updating historical activation.

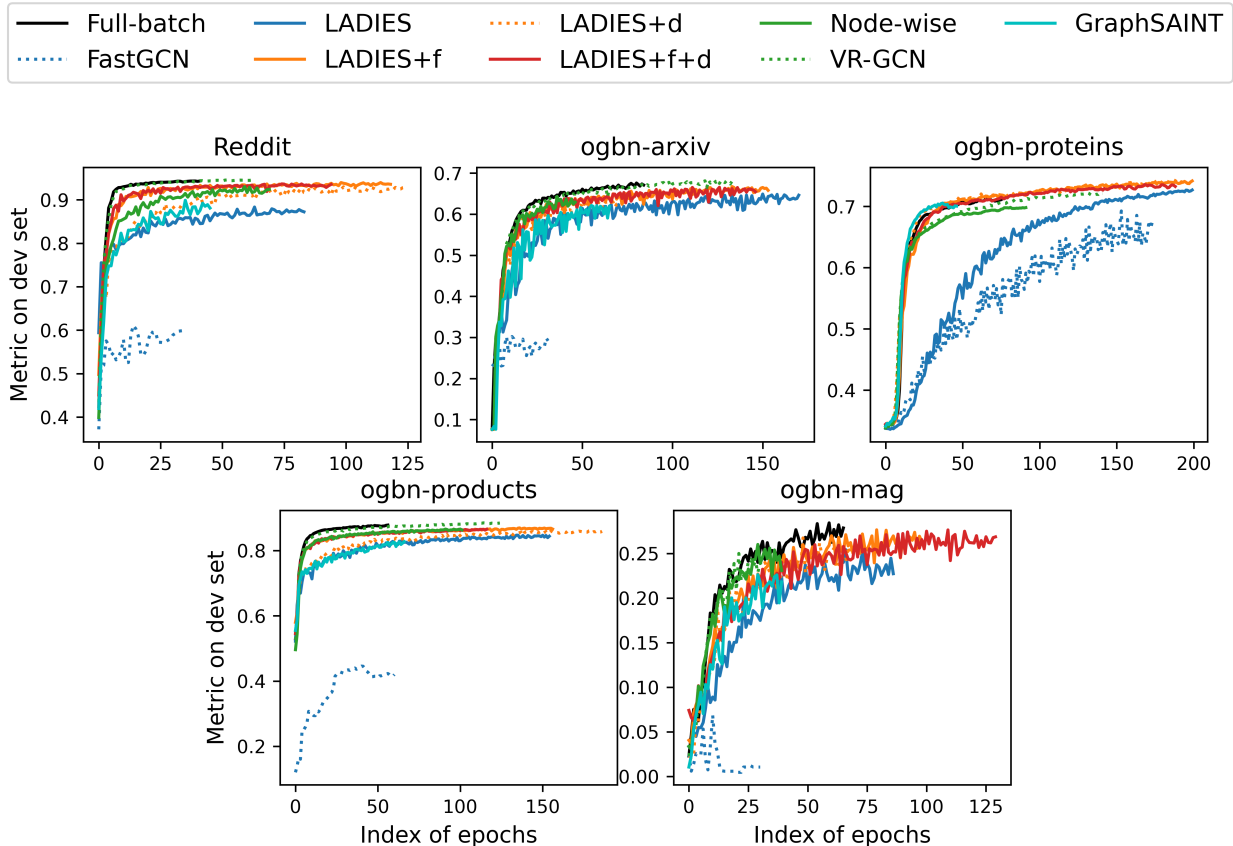


Figure 4: Accuracy metrics of each epoch on the validation set. The layer-wise sampling methods follow the “increasing” setting (denoted with (2) in Table 4); for the node-wise sampling methods, the number of neighbors is 2 per node.

Table 5: Average sampling time (in milliseconds) per batch for layer-wise methods and vanilla node-wise method (GraphSAGE). 512 and 1024 (followed with the dataset name) indicate the number of nodes sampled for one layer. The “f” and “d” in “LADIES+f+d” denotes “flat” and “debiased” respectively.

	FastGCN	LADIES	LADIES+f	LADIES+d	LADIES+f+d	Node-wise
Reddit (512)	10.6 ± 0.9	10.9 ± 0.3	10.0 ± 0.2	13.1 ± 0.3	13.1 ± 0.4	632.5 ± 4.3
Reddit (1024)	10.0 ± 0.6	11.8 ± 0.4	10.4 ± 0.1	17.1 ± 0.4	16.1 ± 0.6	637.0 ± 4.2
arxiv (512)	4.2 ± 0.1	8.3 ± 0.1	7.8 ± 0.1	11.7 ± 0.2	11.7 ± 0.5	585.2 ± 3.6
arxiv (1024)	6.9 ± 0.1	9.7 ± 0.1	9.0 ± 0.1	17.2 ± 0.3	16.5 ± 0.3	585.6 ± 3.1
mag (512)	16.8 ± 0.1	27 ± 0.1	24.5 ± 0.1	30.0 ± 0.03	27.8 ± 0.1	1084.3 ± 1.7
mag (1024)	18.9 ± 0.2	28.6 ± 0.2	27.7 ± 0.1	36.0 ± 0.2	34.9 ± 0.1	1119 ± 2.9
proteins (512)	11.1 ± 1	11.2 ± 0.3	10 ± 0.2	13.6 ± 0.2	12.6 ± 0.2	830.9 ± 5.3
proteins (1024)	8.9 ± 0.2	12.4 ± 0.1	11.4 ± 0.1	18.9 ± 0.2	18.0 ± 0.3	804.2 ± 4.6
products (512)	54.8 ± 0.7	83.4 ± 1.3	80.3 ± 0.4	83.7 ± 0.8	83.5 ± 0.6	2795.4 ± 4.7
products (1024)	57.1 ± 0.5	80.8 ± 0.8	78.7 ± 0.7	87.0 ± 0.6	85.4 ± 0.7	2737.7 ± 4.8

Table 6: Average training time (in milliseconds) per batch for a 2-layer GCN.

	Reddit	ogbn-arxiv	ogbn-mag	ogbn-proteins	ogbn-products
Full-batch	372 ± 21.5	65.2 ± 3.97	72.3 ± 8.25	1702 ± 67.0	703 ± 77.8
Node-wise (2)	8.13 ± 1.12	22.0 ± 3.64	17.3 ± 4.67	9.50 ± 1.29	8.34 ± 1.21
Node-wise (10)	11.3 ± 1.05	19.7 ± 2.84	22.0 ± 5.60	10.3 ± 1.29	11.7 ± 1.31
VR-GCN (2)	153 ± 17.3	86.8 ± 6.09	106 ± 12.4	239 ± 42.7	88.5 ± 2.51
VR-GCN (10)	302 ± 23.9	104 ± 8.47	175 ± 15.1	360 ± 45.6	402 ± 65.3
GraphSAINT	8.23 ± 1.14	23.1 ± 3.26	20.4 ± 5.98	8.34 ± 1.07	8.26 ± 1.11
FastGCN	9.47 ± 1.21	24.1 ± 5.12	23.3 ± 6.27	8.50 ± 1.22	7.43 ± 1.04
LADIES	7.95 ± 1.03	19.3 ± 3.25	16.7 ± 4.54	8.69 ± 1.11	10.3 ± 1.24
w/ flat	7.86 ± 1.04	16.0 ± 2.37	26.1 ± 6.54	9.00 ± 1.21	8.03 ± 1.07
w/ debiased	7.86 ± 1.11	19.1 ± 3.45	19.5 ± 5.67	8.21 ± 1.04	8.44 ± 1.09
w/ flat & debiased	8.01 ± 1.09	14.6 ± 2.59	20.5 ± 5.62	9.06 ± 1.14	8.11 ± 1.09
FastGCN (2)	9.47 ± 1.25	24.9 ± 5.09	20.8 ± 5.71	8.76 ± 1.06	8.34 ± 1.11
LADIES (2)	14.2 ± 4.68	21.0 ± 4.00	22.7 ± 6.05	8.83 ± 1.12	11.2 ± 1.35
w/ flat	8.70 ± 1.13	23.1 ± 4.04	21.9 ± 5.65	10.3 ± 1.24	13.1 ± 1.52
w/ debiased	8.75 ± 1.15	14.0 ± 1.94	16.3 ± 4.64	10.7 ± 1.29	8.54 ± 1.09
w/ flat & debiased	8.12 ± 1.13	21.0 ± 3.60	13.3 ± 4.15	12.5 ± 1.41	8.50 ± 1.15

Table 7: Average training time (in milliseconds) per batch for a 3-layer GCN.

	Reddit	ogbn-arxiv	ogbn-mag	ogbn-proteins	ogbn-products
Full-batch	1042.8 ± 30.1	148 ± 5.8	352.1 ± 11.5	3312.3 ± 82.1	4490.7 ± 102.6
Node-wise (2)	10.9 ± 1.3	27 ± 4.2	17.2 ± 4.3	11.5 ± 1.3	11.5 ± 1.1
Node-wise (10)	77.8 ± 12	34.9 ± 3.3	52.4 ± 6.7	24.6 ± 1.1	50.4 ± 1.1
VR-GCN (2)	379.7 ± 23.6	154.1 ± 12	218.7 ± 16.7	428.9 ± 53	473.6 ± 69.7
VR-GCN (10)	858.1 ± 32	224.9 ± 17.8	488.1 ± 34.7	1618.7 ± 67.3	2075 ± 112.8
GraphSAINT	9.5 ± 1.1	22.6 ± 3.2	21.2 ± 5.6	11.2 ± 1.3	10.5 ± 1.0
FastGCN	16.9 ± 6.3	30.8 ± 4.3	19 ± 4.8	13 ± 1.3	8.9 ± 1.0
LADIES	10.6 ± 1.3	27.6 ± 3.7	19.9 ± 4.8	11.1 ± 1.3	8.9 ± 1.0
w/ flat	10.1 ± 1.1	26.4 ± 3.9	12.1 ± 2.4	10.1 ± 1.2	9.9 ± 1.0
w/ debiased	10.1 ± 1.2	30 ± 4.1	22.5 ± 5.5	10.6 ± 1.2	10.6 ± 1.0
w/ flat & debiased	9.7 ± 1.1	27.1 ± 3.6	15.7 ± 4.3	10.9 ± 1.2	9.3 ± 1.0
FastGCN (2)	9.6 ± 1.2	27.4 ± 4.6	18.9 ± 4.7	9.8 ± 1.2	9.4 ± 1.1
LADIES (2)	10 ± 1.2	29 ± 4.1	19.2 ± 5.1	10.5 ± 1.2	10.2 ± 1.1
w/ flat	16.1 ± 4.9	27.2 ± 3.7	21.4 ± 5.8	10.4 ± 1.1	13.1 ± 1.4
w/ debiased	10.3 ± 1.1	24.7 ± 3.1	23.3 ± 5.8	10.5 ± 1.2	12.4 ± 1.3
w/ flat & debiased	10.7 ± 1.1	26.8 ± 4.4	24.8 ± 6.4	10.5 ± 1.1	9.9 ± 1.1



#### A.4 Additional Regression Experiments and Details

For the regression experiments in Section 4.1, we train a 3-layer GCN with LADIES sampler, with 256 hidden variables per layer. The batch size is 512. Early stopping training policy is applied. We also remark that these experiments are conducted to check the assumption of importance sampling, rather than pursuing SOTA performance. When we finish training the model, the norms of rows in  $\mathbf{HW}$  are extracted through a full-batch inference with all training nodes. The regression lines are fitted with all data points while the scatter plots (Figure 2) only present 1000 randomly sampled points in each layer for the visualization.

Figure 5 and Figure 6 are supplementary to Figure 2, where the scatter plots make use of all points. The former uses full-batch SGD training (without sampling) while the latter still uses LADIES for training. However, they show very similar regression results. The assumption:  $\|(\mathbf{HW})_{[i]}\| \propto \|P^{[i]}\|$  does not hold on all of these datasets. Note that we do not have the regression result on the ogbn-product dataset since the training of 3-layer GCN fails due to the memory limitation.

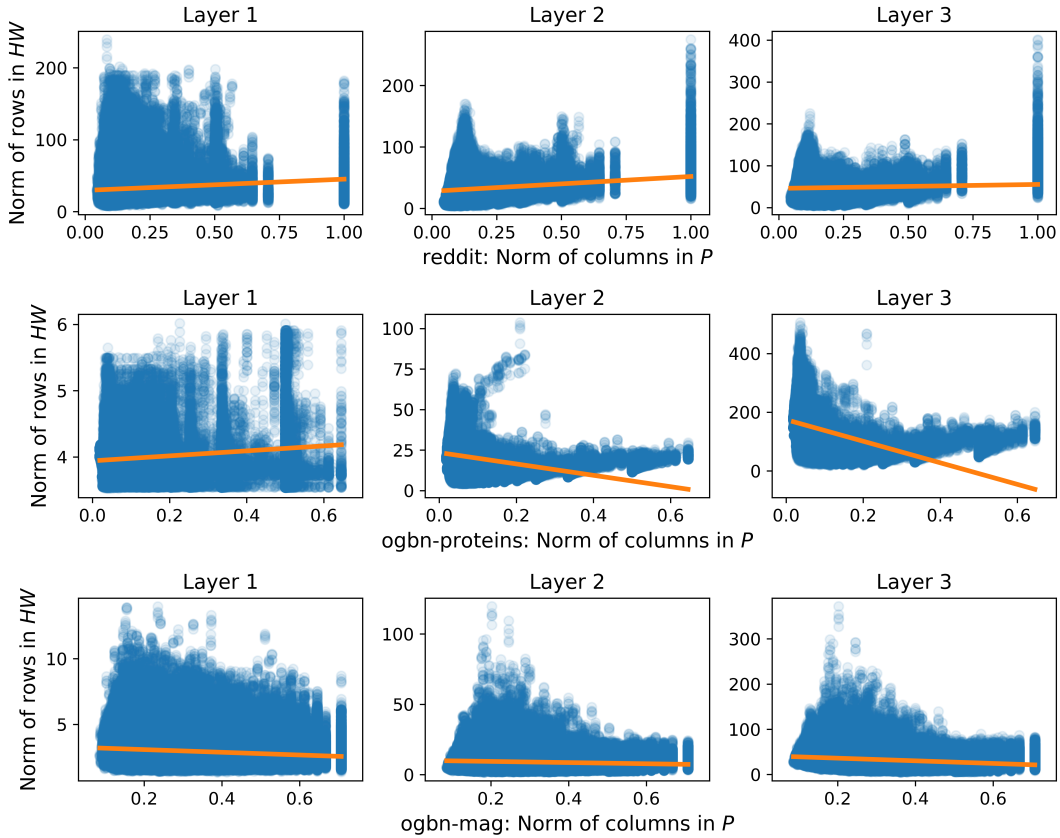


Figure 5: Regression on Reddit, ogbn-protein, ogbn-mag datasets. GCN is trained with full-batch SGD.

## B Time Complexity Analysis

We analyze the complexity of vanilla node-wise sampling and layer-wise sampling in this section. The analysis is adapted from the work by Zou et al. (2019), but we show a lighter bound for layer-wise sampling. For  $l$  such that  $0 \leq l \leq L - 1$ , the propagation formulas for sampling based GCN can be formulated as:

$$\tilde{\mathbf{Z}}^{(l+1)} = \tilde{\mathbf{P}}^{(l)} \tilde{\mathbf{H}}^{(l)} \mathbf{W}^{(l)},$$

where  $\tilde{\mathbf{H}}^{(l)} = \tilde{\mathbf{Z}}^{(l)} \in \mathbb{R}^{s_l \times p}$ ,  $\tilde{\mathbf{P}}^{(l)} \in \mathbb{R}^{s_{l+1} \times s_l}$ ,  $\mathbf{W}^{(l)} \in \mathbb{R}^{p \times p}$ . In particular, for LADIES,  $\tilde{\mathbf{P}}_{LADIES}^{(l)} = \mathbf{Q}^{(l+1)} \mathbf{P} \mathbf{S}^{(l)}$ .

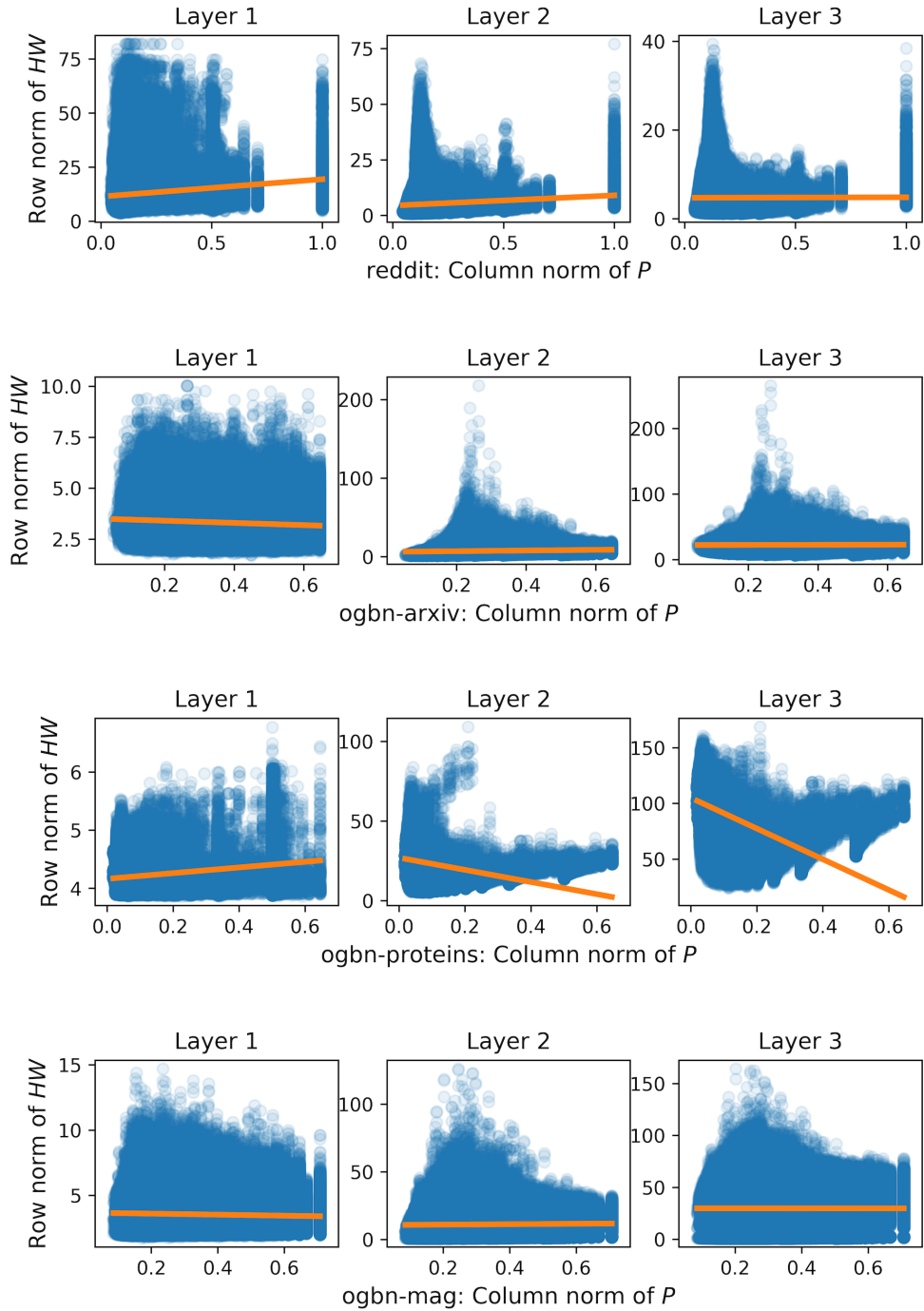


Figure 6: Regression on Reddit, ogbn-arxiv, ogbn-protein, ogbn-mag datasets. GCN is trained by LADIES. The fitted regression line is in orange color.

Table 8: The time complexity for computation for  $L$ -layer GCN training by layer-wise sampling and node-wise sampling . The first column refers to the matrix operation type, nodes aggregation or linear transformation.

	Layer-wise	Node-wise
Nodes Aggregation	$\mathcal{O}(scpL)$	$\mathcal{O}(sb^Lp)$
Linear Transformation	$\mathcal{O}(sp^2L)$	$\mathcal{O}(sb^{L-1}p^2)$

For simplicity, we suppose that the number of hidden variables in each layer is fixed as  $p$ , the same as the dimension of  $\mathbf{H}^{(0)}$ . The batch size and the numbers of nodes sampled in each layer equal are set all equal to a fixed constant  $s$ . We assume the number of sampled neighbors per node in node-wise sampling is  $b$ . We denote the maximal degree of all the nodes in the graph as  $c$ . The computational cost of the propagation comes from two parts: the linear transformation, a dense matrix product,  $\tilde{\mathbf{H}}^{(l)}\mathbf{W}^{(l)}$  and the node aggregation, a sparse matrix product,  $\bar{\mathbf{P}}^{(l)}(\tilde{\mathbf{H}}^{(l)}\mathbf{W}^{(l)})$ . The time complexity is summarized in Table 8. We additionally comment although the time cost of two parts both linearly depend on the number of nodes involved (number of non-zero elements in  $\mathbf{Q}^{(l+1)}$ ), the node aggregation part usually dominates since the sparse matrix product involved is less efficient than the dense matrix product involved in a modern computer.

The linear transformation,  $\tilde{\mathbf{H}}^{(l)}\mathbf{W}^{(l)}$  is dense matrix production. The cost depends on the shape of two matrices, and is given as  $\mathcal{O}(s_l p^2)$ . LADIES fixes  $s_l$  as  $s$  for each layer, so  $\mathcal{O}(s_l p^2) = \mathcal{O}(sp^2)$ . For node-wise sampling  $s_l = sb^{L-l}$ , since number of node exponentially grows. Thus by summation over all the layers, we have the results in the second row in Table 8.

The node aggregation,  $\bar{\mathbf{P}}^{(l)}(\tilde{\mathbf{H}}^{(l)}\mathbf{W}^{(l)})$  is a sparse matrix production, since  $\bar{\mathbf{P}}^{(l)}$  is sparse. For simplicity, we denote  $\tilde{\mathbf{H}}^{(l)}\mathbf{W}^{(l)}$  as  $\mathbf{C}^{(l)} \in \mathbb{R}^{s_l \times p}$ . Thus the time complexity of this sparse matrix production becomes  $\mathcal{O}(nnz^{(P_l)}p)$ , where  $nnz^{(P_l)}$  is the number of non-zero entries in  $\bar{\mathbf{P}}^{(l)}$ . For layer-wise sampling, since we sample  $s$  nodes for each layer and each node has at most  $c$  neighbors, so  $nnz^{(P_l)} \leq sc$ . For node-wise sampling, since each node has  $b$  neighbors and the neighbors are not shared by all the nodes in each layer,  $nnz^{(P_l)} = bs_l = sb^{L+1-l}$ . By summation over all the layers, we attain the results in the first row of Table 8.

## C Theoretical Analysis of Sampling Probabilities

### C.1 Results in approximate matrix multiplication

In this section, we revisit approximate matrix multiplication to derive the previous layer-wise sampling methods. Specifically, the sampling matrix  $\mathbf{S}$  used in FastGCN and LADIES can be decomposed as  $\mathbf{S} = \mathbf{\Pi}\mathbf{\Pi}^T$ , where  $\mathbf{\Pi} \in \mathbb{R}^{n \times d}$  is a sub-sampling sketching matrix defined as follows:

**Definition C.1** (Sub-sampling sketching matrix). *Consider a discrete distribution which draws  $i$  with probability  $p_i > 0, \forall i \in [n]$ . For a random matrix  $\mathbf{\Pi} \in \mathbb{R}^{n \times d}$ , if  $\mathbf{\Pi}$  has i.i.d. columns and each column  $\mathbf{\Pi}^{(j)}$  can randomly be  $\frac{1}{\sqrt{dp_i}}\mathbf{e}_i$  with probability  $p_i$ , where  $\mathbf{e}_i$  is the  $i$ -th column of the  $n$ -by- $n$  identity matrix  $\mathbf{I}_n$ , then  $\mathbf{\Pi}$  is called a sub-sampling sketching matrix with sub-sampling probabilities  $\{p_i\}_{i=1}^n$ .*

With this definition, we introduce a result in AMM to construct the sub-sampling sketching matrix, which coincides with the conclusion in FastGCN and LADIES.

**Theorem C.1** (Theorem 1 (Drineas et al., 2006)). *Suppose  $\mathbf{B} \in \mathbb{R}^{n_B \times n}$ ,  $\mathbf{C} \in \mathbb{R}^{n \times n_C}$ , the number of sub-sampled columns  $d \in \mathbb{Z}^+$  such that  $1 \leq d \leq n$ , and the sub-sampling probabilities  $\{p_i\}_{i=1}^n$  are such that  $\sum_{i=1}^n p_i = 1$  and such that for a quality coefficient  $\beta \in (0, 1]$*

$$p_i \geq \beta \frac{\|\mathbf{B}^{[i]}\| \|\mathbf{C}_{[i]}\|}{\sum_{i'=1}^n \|\mathbf{B}^{[i']}\| \|\mathbf{C}_{[i']}\|}, \forall i \in [n]. \quad (11)$$

*Construct a sub-sampling sketching matrix  $\mathbf{\Pi} \in \mathbb{R}^{n \times d}$  with sub-sampling probabilities  $\{p_i\}_{i=1}^n$  as in Definition C.1, and let  $\mathbf{B}\mathbf{\Pi}\mathbf{\Pi}^T\mathbf{C}$  be an approximation to  $\mathbf{BC}$ . Let  $\delta \in (0, 1)$  and  $\eta = 1 + \sqrt{(8/\beta) \log(1/\delta)}$ . Then*

with probability at least  $1 - \delta$ ,

$$\|\mathbf{BC} - \mathbf{B}\mathbf{\Pi}\mathbf{\Pi}^T\mathbf{C}\|_F^2 \leq \frac{\eta^2}{\beta d} \|\mathbf{B}\|_F^2 \|\mathbf{C}\|_F^2. \quad (12)$$

**Remark.** The theorem is closely related to Lemma 1 in Appendix B of LADIES, which studies the variance  $\mathbb{E} \|\mathbf{BC} - \mathbf{BSC}\|_F^2$ . For the choice of sub-sampling probabilities, Equation (11) reproduces the conclusion in FastGCN and LADIES, when we respectively take  $\mathbf{B}$  as  $\mathbf{P}$  and  $\mathbf{QP}$ .

## C.2 Comparison of Sampling Variance Between Our Sampling Probabilities and LADIES

Whether our choice of probabilities can outperform the LADIES depends on the distribution of the norms of rows in  $\mathbf{HW}$ . When  $\|\mathbf{HW}_{(i)}\|$  is not proportional to the corresponding  $\ell_2$  norm of column  $(\mathbf{QP})^{(i)}$ , our proposed probabilities can benefit the approximate matrix multiplication task more than the ones assuming a relation of proportionality. We find the common long-tail distribution of numbers suffices to exert the strengths of the new probabilities, which can be concluded as the following assumption:

**Assumption 1.** To simplify the notation we denote  $\mathbf{B} := \mathbf{QP}$  and  $\mathbf{C} := \mathbf{HW}$ , where  $\mathbf{P}$  is an  $n$ -by- $n$  matrix as defined above. Let  $m$  be the number of non-zero columns in  $\mathbf{B}$ , and define  $C_1 := \frac{\|\mathbf{B}\|_F^2/m}{(\sum_{i=1}^n \|\mathbf{B}^{[i]}\|/m)^2} \geq 1$ . There also exists a constant  $C_2 \geq 1$  such that  $\frac{1}{C_2} \|\mathbf{C}\|_F^2/n \leq \|\mathbf{C}_{[i]}\|^2 \leq C_2 \|\mathbf{C}\|_F^2/n$ . Assume  $C_1/C_2^2 \geq 1$ .

With the assumption above, we show the variance of the approximation with our proposed probabilities is smaller than the variance of LADIES by the following lemma.

**Lemma C.1.** We denote the sampling matrix with our probabilities in Equation (5) as  $\mathbf{S}_1$ , and denote the sampling matrix with probabilities of LADIES in Equation (2) as  $\mathbf{S}_0$ . If Assumption 1 holds, then we have

$$\mathbb{E} \|\mathbf{BS}_1\mathbf{C} - \mathbf{BC}\|_F^2 \leq \mathbb{E} \|\mathbf{BS}_0\mathbf{C} - \mathbf{BC}\|_F^2.$$

**Remark.** Assumption 1 is related to the uniformity in the distributions of  $\|\mathbf{B}^{[i]}\|$ 's and  $\|\mathbf{C}_{[i]}\|$ 's. We tentatively discuss the implication of the assumption in Appendix C.2. We remark the assumption indicates it is unrealistic that the new probabilities can outperform the ones in LADIES, as distributions of datasets can vary. Nevertheless, as shown in Section 6 it can be an effective attempt to improve the prediction accuracy of LADIES by simply adopting the conservative sampling scheme.

To prove Lemma C.1, we first adapt a technical lemma (Zou et al., 2019, Lemma 1), which relates the sampling matrix to the variance (expectation of squared Frobenius norm) of the approximate matrix multiplication.

**Lemma C.2** (Adapted from Lemma 1 (Zou et al., 2019)). Given two matrices  $\mathbf{B} \in \mathbb{R}^{n_B \times n}$  and  $\mathbf{C} \in \mathbb{R}^{n \times n_C}$ , for any  $i \in [n]$  define the positive probabilities  $p_i$ 's such that  $\sum_{i=1}^n p_i = 1$ . We further require the probability  $p_i = 0$  if and only if the corresponding column  $\mathbf{B}^{[i]}$  or row  $\mathbf{C}_{[i]}$  is all-zero. The sub-sampling sketching matrix  $\mathbf{\Pi} \in \mathbb{R}^{n \times d}$  is generated accordingly. Let  $\mathbf{S} := \mathbf{\Pi}\mathbf{\Pi}^T$ , it holds that

$$\mathbb{E}_{\mathbf{S}} [\|\mathbf{BSC} - \mathbf{BC}\|_F^2] = \frac{1}{d} \left( \sum_{i:p_i>0} \frac{1}{p_i} \|\mathbf{B}^{[i]}\|^2 \cdot \|\mathbf{C}_{[i]}\|^2 - \|\mathbf{BC}\|_F^2 \right)$$

where  $d$  is the number of samples.

With the lemma above, the proof of Lemma C.1 is provided as follows.

*Proof.* Recall the notation in the main paper is simplified as  $\mathbf{B} := \mathbf{QP}$ ,  $\mathbf{C} := \mathbf{HW}$ . As the union of neighbors of nodes in  $\mathbf{Q}$  cannot cover all the nodes, some columns in  $\mathbf{B}$  are all-zero, and we accordingly

define an  $\mathcal{Q}$ -measurable matrix  $\mathbf{L}$  as in Lemma C.2. We have

$$\begin{aligned}\mathbb{E} [\|\mathbf{BS}_1\mathbf{C} - \mathbf{BC}\|_F^2] &= \mathbb{E}_{\mathcal{Q}} [\mathbb{E}_{S_1} (\|\mathbf{BS}_1\mathbf{C} - \mathbf{BC}\|_F^2 | \mathcal{Q})] \\ &= \frac{1}{d} \mathbb{E}_{\mathcal{Q}} \left[ \sum_{i:p_i>0} \frac{1}{p_i} \|\mathbf{B}^{[i]}\|^2 \cdot \|\mathbf{C}_{[i]}\|^2 - \|\mathbf{BC}\|_F^2 \right].\end{aligned}$$

where the second equation holds as we apply Lemma C.2 to the inner expectation in the right-hand side of the first line. Plugging  $p_i \propto \|\mathbf{B}^{[i]}\|$  (Equation (5) in the main paper) into the preceding probabilities  $p_i$ 's, we reach

$$\begin{aligned}\mathbb{E} [\|\mathbf{BS}_1\mathbf{C} - \mathbf{BC}\|_F^2] &= \frac{\mathbb{E}_{\mathcal{Q}} \left[ \left( \sum_{i:p_i>0} \|\mathbf{B}^{[i]}\| \right) \left( \sum_{i:p_i>0} \|\mathbf{B}^{[i]}\| \|\mathbf{C}_{[i]}\|^2 \right) \right]}{d} - \frac{\mathbb{E}_{\mathcal{Q}} [\|\mathbf{BC}\|_F^2]}{d} \\ &= \frac{1}{d} \mathbb{E}_{\mathcal{Q}} \left[ \left( \sum_{i=1}^n \|\mathbf{B}^{[i]}\| \right) \left( \sum_{i=1}^n \|\mathbf{B}^{[i]}\| \|\mathbf{C}_{[i]}\|^2 \right) \right] - \frac{1}{d} \mathbb{E}_{\mathcal{Q}} [\|\mathbf{BC}\|_F^2].\end{aligned}$$

As computed by Zou et al. (2019), the variance of LADIES is similarly given as

$$\mathbb{E} [\|\mathbf{BS}_0\mathbf{C} - \mathbf{BC}\|_F^2] = \frac{1}{d} \mathbb{E}_{\mathcal{Q}} \left[ \left( \sum_{i:p_i>0} \|\mathbf{B}^{[i]}\|^2 \right) \left( \sum_{i:p_i>0} \|\mathbf{C}_{[i]}\|^2 \right) \right] - \frac{1}{d} \mathbb{E}_{\mathcal{Q}} [\|\mathbf{BC}\|_F^2].$$

Consequently, to prove the lemma it suffices to show that

$$\left( \sum_{i:p_i>0} \|\mathbf{B}^{[i]}\| \right) \left( \sum_{i:p_i>0} \|\mathbf{B}^{[i]}\| \|\mathbf{C}_{[i]}\|^2 \right) \leq \left( \sum_{i:p_i>0} \|\mathbf{B}^{[i]}\|^2 \right) \left( \sum_{i:p_i>0} \|\mathbf{C}_{[i]}\|^2 \right), \quad (13)$$

and the inequality above follows with Assumption 1. Specifically, plugging the inequality  $\|\mathbf{C}_{[i]}\|^2 \leq C_2 \|\mathbf{C}\|_F^2/n, \forall i \in [n]$  in the left-hand-side above, we have

$$\left( \sum_{i:p_i>0} \|\mathbf{B}^{[i]}\| \right) \left( \sum_{i:p_i>0} \|\mathbf{B}^{[i]}\| \|\mathbf{C}_{[i]}\|^2 \right) \leq \left( \sum_{i=1}^n \|\mathbf{B}^{[i]}\| \right)^2 \frac{C_2}{n} \|\mathbf{C}\|_F^2 = \frac{m}{C_1} \|\mathbf{B}\|_F^2 \frac{C_2}{nm} m \|\mathbf{C}\|_F^2,$$

in which the last equation comes from the definition  $C_1 := \frac{\|\mathbf{B}\|_F^2/m}{(\sum_{i=1}^n \|\mathbf{B}^{[i]}\|/m)^2}$ . To close the proof, we utilize the inequality  $\frac{1}{C_2} \|\mathbf{C}\|_F^2/n \leq \|\mathbf{C}_{[i]}\|^2$  and bound  $m \|\mathbf{C}\|_F^2$  by  $n C_2 \sum_{i:p_i>0} \|\mathbf{C}_{[i]}\|^2$ . Finally we attain Equation (13) with the core assumption  $\frac{C_1}{C_2} \geq 1$ .  $\diamond$

**Remark.** In Assumption 1 we indeed implicitly assume  $\|\mathbf{B}^{[i]}\|$ 's follow a long-tail distribution that most norms are around the average while a few columns have large norms. The high non-uniformity makes the average of squared norms much larger than the square of averaged norms. For  $\|\mathbf{C}_{[i]}\|$ 's, considering the normalization techniques (such as batch or layer normalization) to stabilize the scale of the parameters, they tend to not vary widely, which implies a small  $C_2$ . The numerical experiments on the comparison of approximation error (see Figure 1) and the histograms of the norms in trained models shown in Figure 7 further validate the assumption. Based on the empirical analysis above, we claim the assumption is mild and tends to hold at least for some datasets.

### C.3 Distributions of the Matrix Rows / Columns Norm

Figure 7 demonstrates the distribution of  $\|\mathbf{P}^{[i]}\|$  and  $\|(\mathbf{HW})_{[i]}\|$  (layer 1, 2, 3) for Reddit, ogbn-arxiv, ogbn-protein and ogbn-mag datasets. The  $\|(\mathbf{HW})_{[i]}\|$ 's are obtained from the experiment in Section A.4. The outliers larger than the 99.9% quantile or small than the 0.1% quantile are removed.

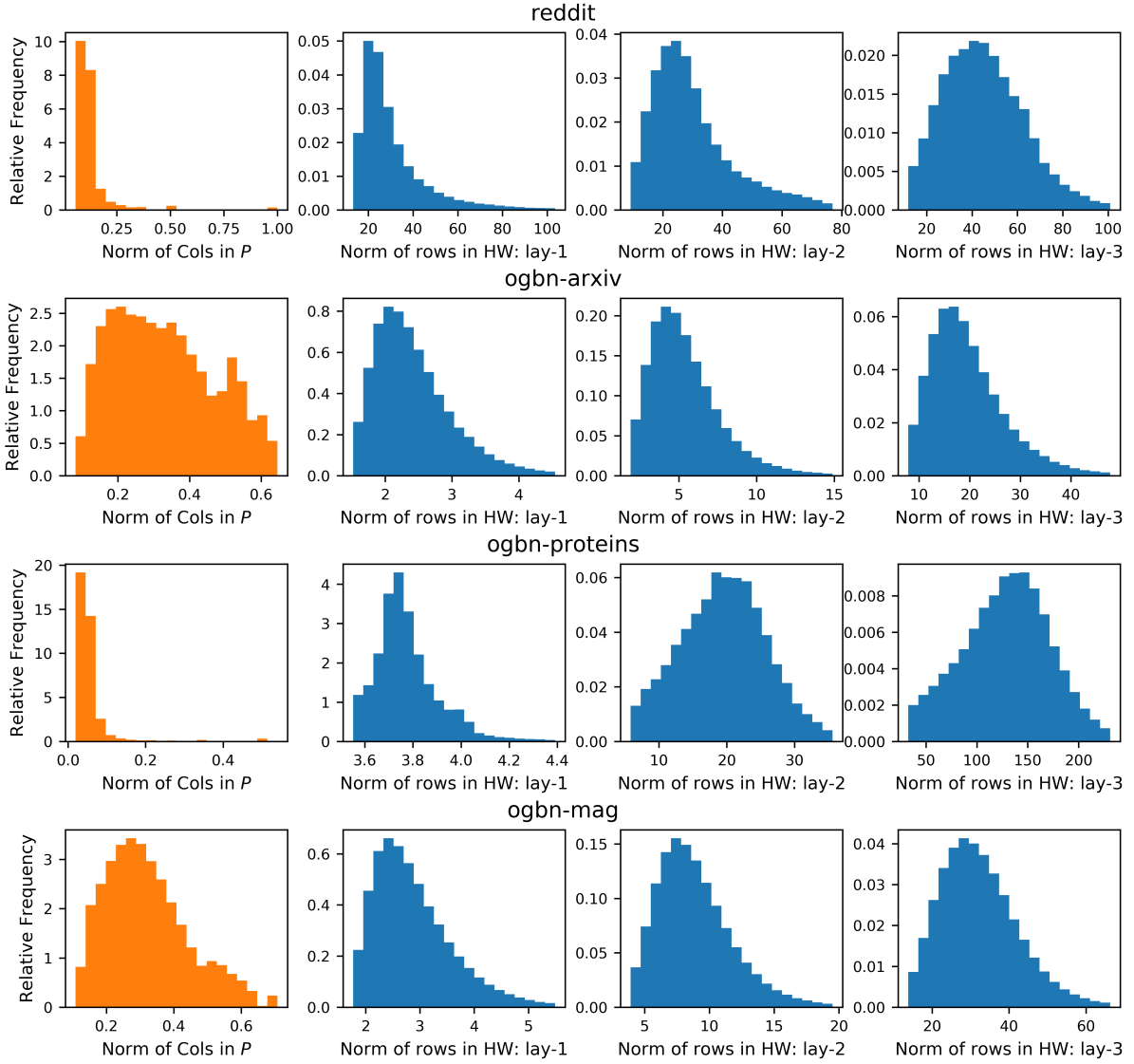


Figure 7: Distribution of  $\|P^{[i]}\|$  and  $\|(HW)_{[i]}\|$  for Reddit, ogbn-arxiv, ogbn-protein and ogbn-mag.



As shown in the histograms, our analysis regarding Assumption 1 tends to hold generally on these datasets. For the norms of columns in  $\mathbf{P}$  (as a replacement for  $\mathbf{QP}$  for clarity), we observe there are some columns with large norms far beyond the average. Those columns contribute a lot to the quadratic mean, which results in a huge  $C_1$  in Assumption 1. In contrast, the norms of rows in  $\mathbf{HW}$  concentrate around their average, inducing a small  $C_2$ . Those facts together with Assumption 1 and Lemma C.1 in the main paper explain why our proposed sampling probabilities are more proper for some real datasets.

#### C.4 Proof for Theorem 1

*Proof.* We first show  $\mathbb{E}\beta_i^{(k)} = 1, \forall i \in [n], k \in [s]$ . As  $\beta_i^{(k)}$  is constructed by Algorithm 1 to attain the unbiased estimator, take  $\mathbf{X}_i = 1, \mathbf{X}_j = 0, \forall j \neq i$ , and we have  $\mathbb{E}\beta_i^{(k)} = \mathbb{E}\sum_{j=1}^n \beta_j^{(k)} \mathbf{X}_j = \sum_{j=1}^n \mathbf{X}_j = 1, \forall i \in [n], k \in [s]$ .

With  $\mathbb{E}\beta_i^{(k+1)}$  at hand, we still need to compute  $\mathbb{E}(\beta_i^{(k+1)})^2$  (and  $\mathbb{E}\beta_i^{(k+1)}\beta_j^{(k+1)}$ ) to obtain the (co)variance. To start the analysis, we recursively write  $\beta_i^{(k+1)}$  as

$$\beta_i^{(k+1)} = \mathbf{1}_{\{i \in S_k\}} [\beta_i^{(k)} (1 - \alpha_{k+1}) + \alpha_{k+1}] + \mathbf{1}_{\{i \notin S_k\}} \mathbf{1}_{\{i \in S_{k+1}\}} \frac{1 - \sum_{j \in S_k} p_j}{p_i} \alpha_{k+1} := \pi_i^{k+1}(\beta_i^{(k)}) + \gamma_i^{(k+1)}.$$

For  $\mathbb{E}(\beta_i^{(k+1)})^2$ , we notice the cross term  $2\pi_i^{k+1}(\beta_i^{(k)})\gamma_i^{(k+1)}$  is always zero as  $\mathbf{1}_{\{i \in S_k\}}\mathbf{1}_{\{i \notin S_k\}} := 0$ ; as for the first terms, utilizing the fact  $\mathbf{1}_{\{i \in S_k\}}\beta_i^{(k)} = \beta_i^{(k)}$  we have

$$\mathbb{E}\left(\pi_i^{k+1}(\beta_i^{(k)})\right)^2 = \mathbb{E}(\beta_i^{(k)})^2(1 - \alpha_{k+1})^2 + 2\alpha_{k+1}(1 - \alpha_{k+1}) + q_i^k \alpha_{k+1}^2,$$

to obtain the last term,

$$\begin{aligned} \mathbb{E}(\gamma_i^{(k+1)})^2 &= \mathbb{E}\mathbb{E}\left(\mathbf{1}_{\{i \notin S_k\}} \mathbf{1}_{\{i \in S_{k+1}\}} \frac{1 - \sum_{j \in S_k} p_j}{p_i} \alpha_{k+1} \mid i \notin S_k\right) \\ &= \mathbb{E}\left[\mathbf{1}_{\{i \notin S_k\}} \mathbb{E}\left(\mathbf{1}_{\{i \in S_{k+1}\}} \frac{1 - \sum_{j \in S_k} p_j}{p_i} \alpha_{k+1} \mid i \notin S_k\right)\right] \\ &= q_i^k \sum_{S_k \not\ni i} \frac{p_{S_k}}{q_i^k} \frac{1 - \sum_{j \in S_k} p_j}{p_i} \alpha_{k+1}^2 = \frac{r_i^k}{p_i} \alpha_{k+1}^2. \end{aligned}$$

For  $\mathbb{E}\beta_i^{(k+1)}\beta_j^{(k+1)}$ , we can similarly drop the last term  $\mathbb{E}\gamma_i^{(k+1)}\gamma_j^{(k+1)}$  as  $\mathbf{1}_{\{i \in S_k\}}\mathbf{1}_{\{j \notin S_k\}} := 0$ ; as for the first term  $\mathbb{E}\pi_i^{k+1}(\beta_i^{(k)})\pi_j^{k+1}(\beta_j^{(k)})$ , we have

$$\mathbb{E}\pi_i^{k+1}(\beta_i^{(k)})\pi_j^{k+1}(\beta_j^{(k)}) = \mathbb{E}\beta_i^{(k)}\beta_j^{(k)}(1 - \alpha_{k+1})^2 + \mathbb{E}\left(\mathbf{1}_{\{i \in S_k\}}\beta_j^{(k)} + \mathbf{1}_{\{j \in S_k\}}\beta_i^{(k)}\right)\alpha_{k+1}(1 - \alpha_{k+1}) + p_{i,j}^k \alpha_{k+1}^2,$$

where  $p_{i,j}^k$  is the probability that **both** index  $i, j$  are in the first  $k$  samples; as for the next term  $\mathbb{E}\pi_i^{k+1}(\beta_i^{(k)})\gamma_j^{(k+1)}$ , we first compute

$$\begin{aligned} \mathbb{E}\beta_i^{(k)}\gamma_j^{(k+1)} &= \mathbb{E}\mathbb{E}\left(\beta_i^{(k)} \mathbf{1}_{\{j \notin S_k\}} \mathbf{1}_{\{j \in S_{k+1}\}} \frac{1 - \sum_{j' \in S_k} p_{j'}}{p_j} \alpha_{k+1} \mid \mathcal{F}_k\right) \\ &= \mathbb{E}\left[\beta_i^{(k)} \mathbf{1}_{\{j \notin S_k\}} \frac{1 - \sum_{j' \in S_k} p_{j'}}{p_j} \alpha_{k+1} \mathbb{E}(\mathbf{1}_{\{j \in S_{k+1}\}} \mid \mathcal{F}_k)\right] \\ &= \mathbb{E}\left[\beta_i^{(k)} \mathbf{1}_{\{j \notin S_k\}} \frac{1 - \sum_{j' \in S_k} p_{j'}}{p_j} \alpha_{k+1} \frac{p_j}{1 - \sum_{j' \in S_k} p_{j'}}\right] = \mathbb{E}\left(\mathbf{1}_{\{j \notin S_k\}} \beta_i^{(k)}\right) \alpha_{k+1}, \end{aligned}$$

and similarly we have

$$\begin{aligned}
\mathbb{E} \mathbf{1}_{\{i \in S_k\}} \gamma_j^{(k+1)} &= \mathbb{E} \mathbb{E} \left( \mathbf{1}_{\{i \in S_k\}} \mathbf{1}_{\{j \notin S_k\}} \mathbf{1}_{\{j \in S_{k+1}\}} \frac{1 - \sum_{j' \in S_k} p_{j'}}{p_j} \alpha_{k+1} | \mathcal{F}_k \right) \\
&= \mathbb{E} \left[ \mathbf{1}_{\{i \in S_k\}} \mathbf{1}_{\{j \notin S_k\}} \frac{1 - \sum_{j' \in S_k} p_{j'}}{p_j} \alpha_{k+1} \mathbb{E} (\mathbf{1}_{\{j \in S_{k+1}\}} | \mathcal{F}_k) \right] \\
&= \mathbb{E} \left[ \mathbf{1}_{\{i \in S_k\}} \mathbf{1}_{\{j \notin S_k\}} \frac{1 - \sum_{j' \in S_k} p_{j'}}{p_j} \alpha_{k+1} \frac{p_j}{1 - \sum_{j' \in S_k} p_{j'}} \right] = \mathbb{E} (\mathbf{1}_{\{j \notin S_k\}} \mathbf{1}_{\{i \in S_k\}}) \alpha_{k+1};
\end{aligned}$$

accordingly we can obtain

$$\mathbb{E} \pi_i^{k+1} (\beta_i^{(k)}) \gamma_j^{(k+1)} = \mathbb{E} (\mathbf{1}_{\{j \notin S_k\}} \beta_i^{(k)}) \alpha_{k+1} (1 - \alpha_{k+1}) + \mathbb{E} (\mathbf{1}_{\{j \notin S_k\}} \mathbf{1}_{\{i \in S_k\}}) \alpha_{k+1}^2,$$

and applying the same derivation as above we have

$$\mathbb{E} \pi_j^{k+1} (\beta_j^{(k)}) \gamma_i^{(k+1)} = \mathbb{E} (\mathbf{1}_{\{i \notin S_k\}} \beta_j^{(k)}) \alpha_{k+1} (1 - \alpha_{k+1}) + \mathbb{E} (\mathbf{1}_{\{i \notin S_k\}} \mathbf{1}_{\{j \in S_k\}}) \alpha_{k+1}^2.$$

Combining all the pieces together, we obtain

$$\begin{aligned}
\mathbb{E} \beta_i^{(k+1)} \beta_j^{(k+1)} &= \mathbb{E} \beta_i^{(k)} \beta_j^{(k)} (1 - \alpha_{k+1})^2 + 2\alpha_{k+1} (1 - \alpha_{k+1}) + (p_{i,j}^k + \mathbb{E} (\mathbf{1}_{\{j \notin S_k\}} \mathbf{1}_{\{i \in S_k\}} + \mathbf{1}_{\{i \notin S_k\}} \mathbf{1}_{\{j \in S_k\}})) \alpha_{k+1}^2 \\
&= \mathbb{E} \beta_i^{(k)} \beta_j^{(k)} (1 - \alpha_{k+1})^2 + 2\alpha_{k+1} (1 - \alpha_{k+1}) + (p_{i,j}^k + \mathbb{E} (\mathbf{1}_{\{j \notin S_k\}} \mathbf{1}_{\{i \in S_k\}} + \mathbf{1}_{\{i \notin S_k\}} \mathbf{1}_{\{j \in S_k\}})) \alpha_{k+1}^2.
\end{aligned}$$

With the derivation above, we have

$$\begin{aligned}
\mathbb{E} (\beta_i^{(k+1)})^2 &= \mathbb{E} (\beta_i^{(k)})^2 (1 - \alpha_{k+1})^2 + 2\alpha_{k+1} (1 - \alpha_{k+1}) + \left( \frac{r_i^{(k)}}{p_i} + q_i^k \right) \alpha_{k+1}^2, \\
\mathbb{E} \beta_i^{(k+1)} \beta_j^{(k+1)} &= \mathbb{E} \beta_i^{(k)} \beta_j^{(k)} (1 - \alpha_{k+1})^2 + 2\alpha_{k+1} (1 - \alpha_{k+1}) + q_{i,j}^k \alpha_{k+1}^2
\end{aligned}$$

where  $q_i^k (= 1 - \bar{q}_i^{(k)})$  is the probability that index  $i$  is in the first  $k$  samples, and similarly  $q_{i,j}^k (= 1 - \bar{q}_{i,j}^{(k)} = q_i^k + q_j^k - p_{i,j}^k)$  is the probability that either index  $i$  or index  $j$  is in the first  $k$  samples. Plugging the expression above into the following identities,

$$\begin{aligned}
\text{Var}(\beta_i^{(k+1)}) &= \mathbb{E} (\beta_i^{(k+1)})^2 - \mathbb{E}^2 (\beta_i^{(k+1)}) \\
\text{Cov}(\beta_i^{(k+1)}, \beta_j^{(k+1)}) &= \mathbb{E} \beta_i^{(k+1)} \beta_j^{(k+1)} - \mathbb{E} \beta_i^{(k+1)} \mathbb{E} \beta_j^{(k+1)},
\end{aligned}$$

we can then have the expression for the covariance stated in the main paper.

For the scale of the covariance, we prove the upper bound through induction. We can verify the upper bounds hold for  $k = 1$ , and for the (co)variance with  $\alpha_k = \frac{1}{k}$ ,  $\text{Var}(\beta_i^{(k+1)})$  and  $\text{Cov}(\beta_i^{(k+1)}, \beta_j^{(k+1)})$  now respectively becomes

$$\begin{aligned}
\text{Var}(\beta_i^{(k+1)}) &= \frac{k^2}{(k+1)^2} \text{Var}(\beta_i^{(k)}) + \left( \frac{r_i^{(k)}}{p_i} - \bar{q}_i^{(k)} \right) \frac{1}{(k+1)^2}, \\
\text{Cov}(\beta_i^{(k+1)}, \beta_j^{(k+1)}) &= \frac{k^2}{(k+1)^2} \text{Cov}(\beta_i^{(k)}, \beta_j^{(k)}) - \bar{q}_{i,j}^{(k)} \frac{1}{(k+1)^2}.
\end{aligned}$$

Utilizing the induction conditions that for all  $i, j$ , we have

$$\begin{aligned}
\text{Var}(\beta_i^{(k)}) &\leq \frac{1}{k} \left( \frac{1}{p_i} - 1 \right), \\
|\text{Cov}(\beta_i^{(k)}, \beta_j^{(k)})| &\leq \frac{1}{k}.
\end{aligned}$$

---

Along with the facts that  $\frac{r_i^{(k)}}{p_i} - \bar{q}_i^{(k)} \leq \frac{\bar{q}_i^{(k)}}{p_i} - \bar{q}_i^{(k)} \leq \frac{1}{p_i} - 1$  and  $\bar{q}_{i,j}^{(k)} \leq 1$ , we can finally achieve the inequality that

$$\begin{aligned}\text{Var}(\beta_i^{(k+1)}) &\leq \frac{1}{k+1} \left( \frac{1}{p_i} - 1 \right), \\ |\text{Cov}(\beta_i^{(k+1)}, \beta_j^{(k+1)})| &\leq \frac{1}{k+1}.\end{aligned}$$

◇

**Remark.** The choice of  $\alpha_k = \frac{1}{k}$  here is mainly for easing the proof, while may not be the optimal choice in practice; indeed in SRS the  $\alpha_k$ 's are different than the ones used here.